AIMS Mathematics, 10(9): 20689–20714.
DOI:10.3934/math.2025924
Received: 12 June 2025
Revised: 24 August 2025
Accepted: 01 September 2025
Published: 09 September 2025

https://www.aimspress.com/journal/Math

Research article

A finite volume element method for the multi-term time fractional reaction-diffusion models with variable coefficients

Jie Zhao[1], **Zhichao Fang**[2,*] **and Jiahuan Ren**[2]

[1] School of Statistics and Mathematics, Inner Mongolia University of Finance and Economics, Hohhot 010070, China

[2] School of Mathematical Sciences, Inner Mongolia University, Hohhot 010030, China

* **Correspondence:** Email: zcfang@imu.edu.cn.

Abstract: In this paper, a fully discrete finite volume element (FVE) scheme is proposed to treat the linear multi-term time fractional reaction-diffusion models with variable coefficients on triangular grids, where the Caputo fractional derivative of time variable is approximated by the $L1$ formula. The existence and uniqueness of solution for the proposed scheme is proved based on the matrix theories, the stability results are derived in detail by using a multi-term fractional Gronwall inequality, and the optimal error estimates under the $L^2(\Omega)$ and $H^1(\Omega)$ norms are also obtained. Owing to the variable coefficients in the models, a special technique should be used to analyze the stability and error estimates. Finally, three numerical examples with different fractional derivative terms are given to validate the feasibility and effectiveness.

Keywords: finite volume element method; $L1$ formula; multi-term time fractional reaction-diffusion model; stability result; optimal error estimate
Mathematics Subject Classification: 65M08, 65M15, 65M60

1. Introduction

In this paper, we focus on solving the multi-term time fractional reaction-diffusion (TFRD) models with variable coefficients as follows:

$$\begin{cases} P(D_t)u(\boldsymbol{x},t) - \mathrm{div}(\mathcal{A}(\boldsymbol{x})\nabla u(\boldsymbol{x},t)) + q(\boldsymbol{x})u(\boldsymbol{x},t) = f(\boldsymbol{x},t), & (\boldsymbol{x},t) \in \Omega \times J, \\ u(\boldsymbol{x},t) = 0, & (\boldsymbol{x},t) \in \partial\Omega \times J, \\ u(\boldsymbol{x},0) = u_0(\boldsymbol{x}), & \boldsymbol{x} \in \Omega, \end{cases} \tag{1.1}$$

where $J = (0,T]$ is the time interval with $0 < T < \infty$, and $\Omega \subset \mathbb{R}^2$ is a bounded convex polygonal domain with the boundary $\partial\Omega$. The reaction coefficient $q(\boldsymbol{x})$, initial data $u_0(\boldsymbol{x})$, and source function

$f(\boldsymbol{x}, t)$ are known functions, and $q(\boldsymbol{x}) \geq 0$, $\forall \boldsymbol{x} \in \bar{\Omega}$. The diffusion coefficient matrix $\mathcal{A}(\boldsymbol{x}) = \{a_{i,j}(\boldsymbol{x})\}_{2\times 2}$ is symmetric and uniformly positive definite, and there exist two constants $\kappa_0 > 0$ and $\kappa_1 > 0$, such that

$$\kappa_0 \boldsymbol{y}^T \boldsymbol{y} \leq \boldsymbol{y}^T \mathcal{A}(\boldsymbol{x}) \boldsymbol{y} \leq \kappa_1 \boldsymbol{y}^T \boldsymbol{y}, \ \forall \boldsymbol{y} \in \mathbb{R}^2, \ \forall \boldsymbol{x} \in \bar{\Omega}.$$

In (1.1), $P(D_t)u(\boldsymbol{x}, t)$ is the multi-term fractional derivative defined as follows:

$$P(D_t)u(\boldsymbol{x}, t) = \sum_{i=1}^{m} b_i D_t^{\alpha_i} u(\boldsymbol{x}, t), \ \ 0 < \alpha_m < \alpha_{m-1} < \cdots < \alpha_1 < 1, \tag{1.2}$$

where $b_i > 0$ $(1 \leq i \leq m)$ are given real numbers and $D_t^{\alpha_i} u(\boldsymbol{x}, t)$ represents the Caputo fractional derivative of time variable

$$D_t^{\alpha_i} u(\boldsymbol{x}, t) = \frac{1}{\Gamma(1-\alpha_i)} \int_0^t \frac{\partial u(\boldsymbol{x}, s)}{\partial s} \frac{\mathrm{d}s}{(t-s)^{\alpha_i}}, \tag{1.3}$$

where $\Gamma(\cdot)$ represents the Gamma function.

Reaction-diffusion models [1, 2] provide a powerful framework for capturing the dynamics of practical phenomena across science and engineering [3–5]. However, it is widely recognized that some anomalous diffusion phenomena no longer follow the Gauss statistical law or the Fick law [6, 7], which have led to the adoption of fractional models to simulate these special phenomena. Currently, fractional calculus and fractional differential equations (FDEs) have been rigorously established as indispensable analytical frameworks for characterizing anomalous systems exhibiting memory effects, non-locality, and hereditary dynamics [8–10]. Moreover, the mathematical modeling of some complex physical phenomena in particular often necessitates multi-term FDEs [11–13], owing to their capacity to incorporate coupled nonlocal memory effects through multiple fractional calculus or derivative terms.

In recent years, various numerical methods have been employed to solve the multi-term FDEs. Ren and Sun [14] constructed a compact alternating direction implicit (ADI) difference scheme to solve the multi-term time fractional diffusion-wave model. Jin et al. [15] proposed a finite element (FE) method to solve the multi-term time-fractional diffusion equation with smooth and nonsmooth data. Bhrawy and Zaky [16] constructed a spectral tau method to solve multi-term time-space fractional partial differential equations. Qiao and Xu [17] designed an orthogonal spline collocation scheme to solve the multi-term time fractional diffusion problem. Zeng et al. [18] constructed a second-order formula to solve the multi-term FDEs with mooth and non-smooth solutions by introducing appropriate correction terms. Zhao et al. [19] constructed a fully discrete FE scheme to solve the multi-term time fractional diffusion models, and obtained the superconvergence result. Li et al. [20] constructed mixed finite element (MFE) schemes based on the $L1$ formula [21, 22] to solve the multi-term time fractional diffusion and diffusion-wave models. Ezz-Eldien et al. [23] proposed a time-space spectral collocation method to solve the multi-term time fractional mixed sub-diffusion and diffusion-wave model. Liu et al. [24] proposed a Legendre spectral method to solve the multi-term time-fractional mixed diffusion and diffusion-wave model. Shi et al. [25] constructed a fully discrete FE scheme to solve the multi-term time fractional diffusion-wave equations with variable coefficient based on the Crank-Nicolson scheme. Yin et al. [26] designed efficient time-stepping methods to solve multi-term time fractional reaction-diffusion-wave models. She et al. [27] proposed a Chebyshev spectral method to solve the multi-term

time-fractional diffusion equation by using the modified $L1$ formula. Li et al. [28] constructed an ADI difference scheme to solve the multi-term time fractional diffusion equation. Zhao et al. [29] proposed an MFE method based on the Raviart-Thomas MFE space to solve the multi-term TFRD models. Lu et al. [30] designed a physics-informed operator learning framework to solve multi-term time fractional mixed diffusion-wave models. Here, we will apply the finite volume element (FVE) method to solve the multi-term TFRD models with variable coefficients.

The FVE method [31–33] has been extensively applied across diverse scientific disciplines and engineering domains owing to its preservation of local conservation laws for some certain physical quantities, which is very important in practical applications and has attracted the attention of many scholars. Notably, recent advancements in solving FDEs through FVE numerical frameworks have produced particularly noteworthy research contributions. Sayevand and Arjang [34] constructed a spatially semi-discrete FVE scheme to solve the time fractional sub-diffusion equation with the Caputo fractional derivative. Karaa et al. [35] proposed FVE methods to solve the fractional sub-diffusion equation with the Riemann-Liouville fractional derivative, and obtained convergence and superconvergence results. Karaa and Pani [36] designed two FVE schemes to solve the time fractional diffusion problem with smooth and nonsmooth data. Fang et al. [37] proposed a two-grid mixed FVE method to solve the nonlinear TFRD equations by using the $L1$ formula. Wang et al. [38] constructed a mixed FVE scheme to solve the time-fractional damping beam vibration problem. Fang et al. [39] proposed a fully discrete FVE method to solve the TFRD equations by using the $L1$ formula. Fang et al. [40] designed a fast FVE algorithm based on the time two-mesh method to solve the nonlinear time-fractional coupled diffusion model by using the weighted and shifted Grünwald difference (WSGD) formula. Donatelli et al. [41] constructed a fully discrete FVE scheme to solve the conservative steady-state two-sided fractional diffusion model on the generic non-uniform mesh. Zhang and Yang [42] proposed an FVE method to solve the time fractional generalized Burgers' equation. Zhao et al. [43] constructed a mixed FVE scheme combined with the WSGD formula to solve nonlinear time fractional fourth-order reaction-diffusion models. Fang et al. [44] proposed fast two-grid FVE algorithms based on the Crank-Nicolson scheme to solve the nonlinear time fractional mobile/immobile transport model.

In this paper, our primary objective is to construct a fully discrete FVE scheme based on the $L1$ formula to solve the multi-term TFRD models with variable coefficients, and provide relevant numerical theoretical analysis. We first introduce the primal and dual partitions for the space domain Ω, adopt the appropriate *trial* and *test* function spaces, and establish the fully discrete FVE scheme by introducing the interpolation operator Π_h^*. In terms of theoretical analysis of the proposed method, we prove the existence and uniqueness of solution for the FVE scheme by using the matrix theories, and give the stability results and optimal error estimates for u at every discrete time t_n in the $L^2(\Omega)$ and $H^1(\Omega)$ norms. The main contribution of this paper is to use the special technique derived from [39] and the multi-term fractional Gronwall inequality [29] to overcome the theoretical challenges arising from the asymmetry of $a(\cdot, \Pi_h^*\cdot)$ caused by variable coefficients. Finally, we give three numerical examples to validate the effectiveness and convergence accuracy of the proposed FVE method.

The rest of the paper is organized as follows. By using the $L1$ formula and operator Π_h^*, a fully discrete FVE scheme for solving the multi-term TFRD models is constructed in Section 2. In Section 3, we give the proof of the existence and uniqueness of solution for the FVE scheme based on the matrix theories. The stability and optimal error estimate results are given in Sections 4 and 5, respectively. Some numerical results with different fractional derivative term are given to demonstrate the feasibility

and effectiveness in Section 6. In addition, the notation C is represented as a generic positive constant, which does not depend on grid parameters and could have different values at different occurrences.

2. FVE scheme

We first introduce the general Sobolev space $W^{m,p}(\Omega)$ (see [45]) defined in Ω with the norm $\|\cdot\|_{W^{m,p}}$ (abbreviated as $\|\cdot\|_{m,p}$), where $m \geq 0$ and $1 \leq p \leq \infty$. When $p = 2$, it is common practice to denote $H^m(\Omega) = W^{m,2}(\Omega)$ with the norm $\|\cdot\|_{H^m(\Omega)}$ (abbreviated as $\|\cdot\|_m$), and denote $L^2(\Omega) = H^0(\Omega)$ with the norm $\|\cdot\|$ and the inner product $(\cdot,\cdot)$. It is also conventional to use $H_0^1(\Omega) = \{v \in H^1(\Omega) : v|_{\partial\Omega} = 0\}$. Moreover, we also need to use the function space $L^\infty(J; W^{m,p}(\Omega)) = \{v(t) \in W^{m,p}(\Omega) : \operatorname{ess\,sup}_{t\in J}\|v(t)\|_{m,p} < \infty\}$, and denote $L^\infty(W^{m,p}(\Omega)) = L^\infty(J; W^{m,p}(\Omega))$, such as $L^\infty(L^2(\Omega))$ and $L^\infty(H^1(\Omega))$.

Next, we select the $L1$ formula to approximate the multi-term Caputo time fractional derivative. For the time interval $\bar{J} = [0, T]$, we take an equidistant partition $0 = t_0 < t_1 < \cdots < t_N = T$, where $t_n = n\tau$, $\tau = T/N$ with a positive integer N, and $n = 0, 1, \cdots, N$. Let $\phi^n = \varphi(t_n)$ and $\partial_\tau \phi^n = \frac{\phi^n - \phi^{n-1}}{\tau}$ for a known function ϕ on $[0, T]$. From [21, 22], for the fractional parameter α_i, $i = 1, 2, \cdots, m$, we approximate the fractional derivative $D_t^{\alpha_i} u(\boldsymbol{x}, t)$ at time $t = t_n$ as follows:

$$\begin{aligned} D_t^{\alpha_i} u(\boldsymbol{x}, t_n) &= \frac{1}{\Gamma(1-\alpha_i)} \int_0^{t_n} \frac{\partial u(\boldsymbol{x}, s)}{\partial s} \frac{\mathrm{d}s}{(t_n - s)^{\alpha_i}} \\ &= \frac{1}{\Gamma(2-\alpha_i)} \sum_{k=0}^{n-1} \partial_\tau u^{k+1} \Big[(t_n - t_k)^{1-\alpha_i} - (t_n - t_{k+1})^{1-\alpha_i} \Big] + R_{\alpha_i}^n(\boldsymbol{x}) \\ &= \frac{1}{\Gamma(2-\alpha_i)} \Big[d_{\alpha_i,1}^n u^n + \sum_{k=1}^{n-1} (d_{\alpha_i,k+1}^n - d_{\alpha_i,k}^n) u^{n-k} - d_{\alpha_i,n}^n u^0 \Big] + R_{\alpha_i}^n(\boldsymbol{x}) \\ &= \frac{1}{\Gamma(2-\alpha_i)} \sum_{k=0}^{n} \tilde{d}_{\alpha_i,k}^n u^k + R_{\alpha_i}^n(\boldsymbol{x}), \end{aligned} \tag{2.1}$$

where $\tilde{d}_{\alpha_i,n}^n = d_{\alpha_i,1}^n$, $\tilde{d}_{\alpha_i,k}^n = d_{\alpha_i,n-k+1}^n - d_{\alpha_i,n-k}^n$ $(0 < k \leq n-1)$, $\tilde{d}_{\alpha_i,0}^n = -d_{\alpha_i,n}^n$, $d_{\alpha_i,k}^n = \frac{(t_n - t_{n-k})^{1-\alpha_i} - (t_n - t_{n-k+1})^{1-\alpha_i}}{\tau}$, and denote $D_N^{\alpha_i} u^n = \frac{1}{\Gamma(2-\alpha_i)} \sum\limits_{k=0}^{n} \tilde{d}_{\alpha_i,k}^n u^k$, then we have

$$D_t^{\alpha_i} u(\boldsymbol{x}, t_n) = D_N^{\alpha_i} u^n + R_{\alpha_i}^n(\boldsymbol{x}),\ i = 1, 2, \cdots, m, \tag{2.2}$$

where $R_{\alpha_i}^n(\boldsymbol{x})$ is the truncation error. Then we rewrite (2.1) at $t = t_n$ as follows:

$$\sum_{i=1}^{m} b_i D_N^{\alpha_i} u^n - \operatorname{div}(\mathcal{A}\nabla u^n) + q u^n = f^n - \sum_{i=1}^{m} b_i R_{\alpha_i}^n. \tag{2.3}$$

We introduce the primal grid $\mathcal{T}_h$ and dual grid $\mathcal{T}_h^*$ for the domain Ω. Let $\mathcal{T}_h = \{K\}$ be a quasi-uniform triangular grid with the maximum diameter $h = \max\{h_K\}$, and denote Z_h as the set of all vertices in $\mathcal{T}_h$. Observing Figures 1 (see [40]), for a node $z_0 \in Z_h^0$ with its immediate nodes z_j $(j = 1, 2, \ldots, k)$, we set M_j as the midpoint of the edge $\overline{z_0 z_j}$, choose a point Q_j (such as barycenter in Figure 1(a) or circumcenter in Figure 1(b)) in a triangle $\triangle z_0 z_j z_{j+1}$ with $z_{k+1} = z_1$, then construct a *control volume* $K_{z_0}^*$

by connecting $M_1, Q_1, \ldots, M_k, Q_k, M_1$. Moreover, if z_0 is a boundary node, we can similarly construct the corresponding control volume.

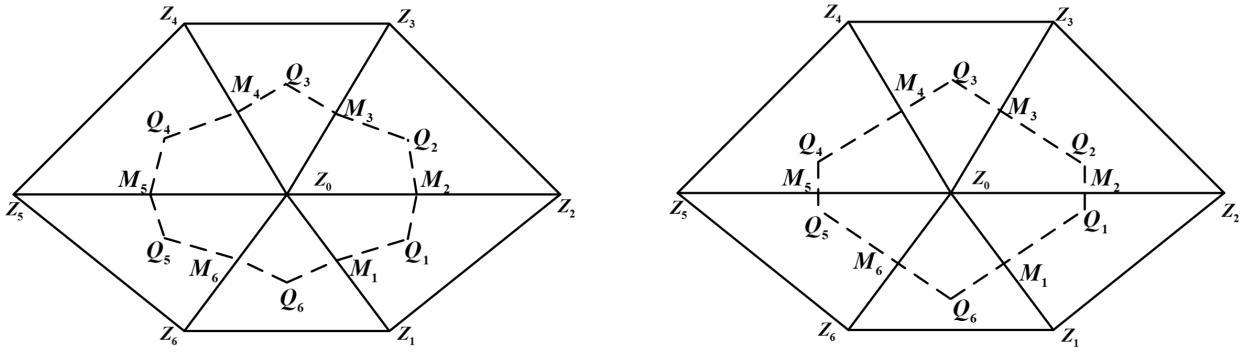

Figure 1. (a) barycenter dual element; (b) circumcenter dual element.

Then we choose the *trial* function space U_h defined by

$$U_h = \{v \in H_0^1(\Omega) : v|_K \in P_1(K),\ \forall K \in \mathcal{T}_h\}, \tag{2.4}$$

and choose the *test* function space U_h^* defined by

$$U_h^* = \{v \in L^2(\Omega) : v|_{K_z^*} \in P_0(K_z^*),\ \forall K_z^* \in \mathcal{T}_h^*,\ \text{and } v|_{\partial\Omega} = 0\}. \tag{2.5}$$

We denote $U_h = \text{span}\{\Phi_z(\boldsymbol{x}) : z \in Z_h^0\}$ and $U_h^* = \text{span}\{\Psi_z(\boldsymbol{x}) : z \in Z_h^*\}$, where Φ_z is the standard linear basis function with the node z, and Ψ_z is the characteristic function of the control volume K_z^*. Let $\Pi_h : C(\Omega) \to U_h$ and $\Pi_h^* : C(\Omega) \to U_h^*$ be two interpolation operators defined by

$$\Pi_h v(\boldsymbol{x}) = \sum_{z \in Z_h^0} v(z)\Phi_z(\boldsymbol{x}), \tag{2.6}$$

$$\Pi_h^* v(\boldsymbol{x}) = \sum_{z \in Z_h^0} v(z)\Psi_z(\boldsymbol{x}). \tag{2.7}$$

From [32], we have

$$\|v - \Pi_h v\|_j \le Ch^{2-j}\|v\|_2,\ j = 0, 1,\ \forall v \in H^2(\Omega), \tag{2.8}$$

$$\|v - \Pi_h^* v\| \le Ch\|v\|_1,\ \forall v \in H^1(\Omega). \tag{2.9}$$

Now, for a vertex $z \in Z_h$, integrating (2.3) on the corresponding control volume K_z^*, and making use of the Green formula and operator Π_h^*, we obtain

$$\int_{K_z^*} \sum_{i=1}^{m} b_i D_N^{\alpha_i} u^n \mathrm{d}\boldsymbol{x} - \int_{\partial K_z^*} \mathcal{A}\nabla u^n \cdot \boldsymbol{n} \mathrm{d}s + \int_{K_z^*} q u^n \mathrm{d}\boldsymbol{x} = \int_{K_z^*} f^n \mathrm{d}\boldsymbol{x} - \int_{K_z^*} \sum_{i=1}^{m} b_i R_{\alpha_i}^n \mathrm{d}\boldsymbol{x}, \tag{2.10}$$

where $\boldsymbol{n}$ stands for the outer-normal direction on ∂K_z^*. Apply the operator Π_h^* to rewrite (2.10) as follows:

$$(\sum_{i=1}^{m} b_i D_N^{\alpha_i} u^n, \Pi_h^* v_h) + a(u^n, \Pi_h^* v_h) = (f^n, \Pi_h^* v_h) - (\sum_{i=1}^{m} b_i R_{\alpha_i}^n, \Pi_h^* v_h),\ \forall v_h \in U_h, \tag{2.11}$$

where $a(\cdot, \Pi_h^*\cdot)$ is defined by

$$a(\bar{u}, \Pi_h^* v_h) = -\sum_{z\in Z_h} v_h(z) \int_{\partial K_z^*} \mathcal{A}\nabla\bar{u}\cdot\boldsymbol{n}\mathrm{d}s + \sum_{z\in Z_h}\int_{\partial K_z^*} q\bar{u}\Pi_h^* v_h \mathrm{d}\boldsymbol{x},\ \bar{u}\in H_0^1(\Omega), v_h\in U_h. \tag{2.12}$$

Let u_h^n be the discrete solution of u at $t = t_n$. We can obtain the fully discrete FVE scheme: find $u_h^n \in U_h,\ n = 1, 2, \cdots, N$, such that

$$(\sum_{i=1}^{m} b_i D_N^{\alpha_i} u_h^n, \Pi_h^* v_h) + a(u_h^n, \Pi_h^* v_h) = (f^n, \Pi_h^* v_h),\ \forall v_h \in U_h, \tag{2.13}$$

where $u_h^0 = P_h u_0$, P_h is the elliptic projection operator defined in Section 5.

3. Existence and uniqueness

In this section, we first give some relevant properties about the bilinear forms $(\cdot, \Pi_h^*\cdot)$ and $a(\cdot, \Pi_h^*\cdot)$.

Lemma 3.1. *[32] For the bilinear form $(\cdot, \Pi_h^*\cdot)$, the following property holds:*

$$(v_h, \Pi_h^* w_h) = (w_h, \Pi_h^* v_h),\ \forall v_h, w_h \in U_h. \tag{3.1}$$

Moreover, there exist two constants $\beta_1 > 0$ and $\beta_2 > 0$ independent of h such that

$$(w_h, \Pi_h^* w_h) \geq \beta_1 \|w_h\|^2,\ \forall w_h \in U_h, \tag{3.2}$$
$$(\phi, \Pi_h^* w_h) \leq \beta_2 \|\phi\|\cdot\|w_h\|,\ \forall \phi \in L^2(\Omega), \forall w_h \in U_h. \tag{3.3}$$

Lemma 3.2. *[32, 46] There exists a constant $\beta_3 > 0$ such that*

$$|a(v_h, \Pi_h^* w_h) - a(v_h, \Pi_h^* w_h)| \leq \beta_3 h \|v_h\|_1 \cdot \|w_h\|_1,\ \forall v_h, w_h \in U_h. \tag{3.4}$$

Lemma 3.3. *[32, 46] There exist three positive constants h_0, β_4, and β_5 such that, for $0 < h \leq h_0$*

$$a(v_h, \Pi_h^* v_h) \geq \beta_4 \|v_h\|_1^2,\ \forall v_h \in U_h, \tag{3.5}$$
$$a(v_h, \Pi_h^* w_h) \leq \beta_5 \|v_h\|_1 \cdot \|w_h\|_1,\ \forall v_h, w_h \in U_h. \tag{3.6}$$

Theorem 3.1. *Assume that $\{u_h^j\}_{j=0}^{n-1}$ are given, then there exists a unique solution u_h^n for the proposed FVE scheme* (2.13).

Proof. Let $U_h = \mathrm{span}\{\Phi_1, \Phi_2, \cdots, \Phi_{M_Z}\}$. Then, $u_h^n \in U_h$ can be expanded as follows:

$$u_h^n(\boldsymbol{x}) = \sum_{j=1}^{M_Z} u_j^n \Phi_j(\boldsymbol{x}). \tag{3.7}$$

Substituting (3.7) into the FVE scheme (2.13), and taking $v_h = \Phi_j$ $(j = 1, 2, \cdots, M_Z)$, we get

$$\sum_{i=1}^{m} \frac{b_i}{\Gamma(2-\alpha_i)} \tilde{d}_{\alpha_i,n}^n B U^n + C U^n = F^n - \sum_{i=1}^{m} \frac{b_i}{\Gamma(2-\alpha_i)} \sum_{k=0}^{n-1} \tilde{d}_{\alpha_i,k}^n B U^k, \tag{3.8}$$

where

$$U^n = (u_1^n, u_2^n, \cdots, u_{M_Z}^n)^T, \qquad B = ((\Phi_i, \Pi_h^* \Phi_j))_{i,j=1,\cdots,M_Z},$$
$$C = (a(\Phi_i, \Pi_h^* \Phi_j))_{i,j=1,\cdots,M_Z}, \quad F^n = ((f(t_n), \Pi_h^* \Phi_j))_{j=1,\cdots,M_Z}^T.$$

From Lemma 3.1, it is easy to know that B is a symmetric positive definite matrix. Let $D = \sum_{i=1}^{m} \frac{b_i}{\Gamma(2-\alpha_i)} \tilde{d}_{\alpha_i,n}^n B + C$, then (3.8) can be rewritten as follows:

$$DU^n = F^n - \sum_{i=1}^{m} \frac{b_i}{\Gamma(2-\alpha_i)} \sum_{k=0}^{n-1} \tilde{d}_{\alpha_i,k}^n B U^k. \tag{3.9}$$

Applying Lemma 3.3, for $\forall Y = (y_1, y_2, \cdots, y_{M_Z})^T \in R^{M_Z} \setminus \{\mathbf{0}\}$, we obtain

$$\begin{aligned} Y^T DY &= \sum_{i=1}^{m} \frac{b_i}{\Gamma(2-\alpha_i)} \tilde{d}_{\alpha_i,n}^n Y^T BY + Y^T CY \\ &= \sum_{i=1}^{m} \frac{b_i}{\Gamma(2-\alpha_i)} \tilde{d}_{\alpha_i,n}^n (z_h, \Pi_h^* z_h) + a(z_h, \Pi_h^* z_h) \\ &\geq \sum_{i=1}^{m} \frac{b_i}{\Gamma(2-\alpha_i)} \tilde{d}_{\alpha_i,n}^n \beta_1 \|z_h\|^2 + \beta_4 \|z_h\|_1^2 > 0, \end{aligned} \tag{3.10}$$

where $z_h = \sum_{i=1}^{M_Z} y_i \Phi_i \neq 0$. It can be seen that $Y^T DY$ (for $Y \in R^{M_Z}$) is a positive definite quadratic form, which is generated by the nonsymmetric matrix D. From [39], we know that D is invertible, and then the linear equations (3.8) possess a unique solution. This conclusion directly implies that the fully discrete FVE scheme (2.13) possesses a unique solution. □

4. Stability analysis

In this section, we aim to present the stability results for the fully discrete FVE scheme (2.13), and first give two important lemmas.

Lemma 4.1. *For a function sequence $\{\varphi^n\}_{k=0}^N$ on U_h and each α_i, $i = 1, 2, \cdots, m$, it follows that*

$$\begin{aligned} &a\Big(\varphi^n, \Pi_h^*\Big(\sum_{k=0}^{n} \tilde{d}_{\alpha_i,k}^n \varphi^k\Big)\Big) \\ =&\frac{1}{2}\Big[\tilde{d}_{\alpha_i,n}^n a(\varphi^n, \Pi_h^* \varphi^n) + \sum_{k=0}^{n-1} \tilde{d}_{\alpha_i,k}^n a(\varphi^k, \Pi_h^* \varphi^k) - \sum_{k=0}^{n-1} \tilde{d}_{\alpha_i,k}^n a(\varphi^n - \varphi^k, \Pi_h^*(\varphi^n - \varphi^k))\Big] \\ &+ \frac{1}{2} \sum_{k=0}^{n-1} \tilde{d}_{\alpha_i,k}^n \Big[a(\varphi^n, \Pi_h^* \varphi^k) - a(\varphi^k, \Pi_h^* \varphi^n)\Big]. \end{aligned} \tag{4.1}$$

Proof. Noting that $\tilde{d}^n_{\alpha_i,n} = -\sum\limits_{k=0}^{n-1} \tilde{d}^n_{\alpha_i,k}$, we have

$$\begin{aligned}
&a\Big(\varphi^n, \Pi_h^*\Big(\sum_{k=0}^{n} \tilde{d}^n_{\alpha_i,k}\varphi^k\Big)\Big)\\
=&\frac{1}{2}\tilde{d}^n_{\alpha_i,n}a(\varphi^n, \Pi_h^*\varphi^n) + \frac{1}{2}\tilde{d}^n_{\alpha_i,n}a(\varphi^n, \Pi_h^*\varphi^n) + \sum_{k=0}^{n-1} \tilde{d}^n_{\alpha_i,k}a(\varphi^n, \Pi_h^*\varphi^k)\\
=&\frac{1}{2}\Big[\tilde{d}^n_{\alpha_i,n}a(\varphi^n, \Pi_h^*\varphi^n) - \sum_{k=0}^{n-1} \tilde{d}^n_{\alpha_i,k}a(\varphi^n, \Pi_h^*\varphi^n) + 2\sum_{k=0}^{n-1} \tilde{d}^n_{\alpha_i,k}a(\varphi^n, \Pi_h^*\varphi^k)\Big].
\end{aligned} \tag{4.2}$$

Observing that

$$\begin{aligned}
-a(\varphi^n, \Pi_h^*\varphi^n) + 2a(\varphi^n, \Pi_h^*\varphi^k) =&a(\varphi^k, \Pi_h^*\varphi^k) - a(\varphi^n - \varphi^k, \Pi_h^*(\varphi^n - \varphi^k))\\
&+ a(\varphi^n, \Pi_h^*\varphi^k) - a(\varphi^k, \Pi_h^*\varphi^n),
\end{aligned} \tag{4.3}$$

and substituting this identity equation into (4.2), we obtain (4.1) and complete the proof. □

Lemma 4.2 ([29]). *Assume that a nonnegative sequence* $\{\varphi^k\}_{k=0}^N$*, a nondecreasing positive sequence* $\{\xi^k\}_{k=0}^N$*, and a constant* $C_0 \geq 1$ *satisfy*

$$\sum_{i=1}^{m} \frac{b_i}{\Gamma(2-\alpha_i)}\tilde{d}^n_{\alpha_i,n}\varphi^n \leq -C_0\sum_{i=1}^{m} \frac{b_i}{\Gamma(2-\alpha_i)}\sum_{k=0}^{n-1} \tilde{d}^n_{\alpha_i,k}\varphi^k + \xi^n,\ 1 \leq n \leq N. \tag{4.4}$$

Then, it follows that

$$\varphi^n \leq C_0^n\Big(\varphi^0 + \frac{1}{\sum\limits_{i=1}^{m} \frac{b_i}{\Gamma(2-\alpha_i)}d^n_{\alpha_i,n}}\xi^n\Big),\ 1 \leq n \leq N. \tag{4.5}$$

Furthermore, it can be further derived that

$$\varphi^n \leq C_0^n\Big(\varphi^0 + \sum_{i=1}^{m} \frac{\Gamma(1-\alpha_i)t_n^{\alpha_i}}{b_i}\xi^n\Big),\ 1 \leq n \leq N. \tag{4.6}$$

We next shall discuss the stability for the fully discrete FVE scheme (2.13).

Theorem 4.1. *Let* $\{u_h^n\}_{n=1}^N$ *be the solution of the FVE scheme* (2.13)*, then we have*

$$\|u_h^n\| \leq \sqrt{\frac{\beta_2}{\beta_1}}\|u_h^0\| + \frac{\beta_2}{\sqrt{2\beta_1\beta_4}}\Big(\sum_{i=1}^{m} \frac{\Gamma(1-\alpha_i)t_n^{\alpha_i}}{b_i}\Big)^{1/2} \sup_{t\in[0,T]}\|f(t)\|. \tag{4.7}$$

Moreover, let $M_0 > 0$ be a constant, then there exists an integer $N_0 > 0$ independent of N and h such that, if $h \leq M_0/N \leq M_0/N_0$ and $h \leq \min\{h_0, h_1\}$, then we have

$$\|u_h^n\|_1 \leq e^{\frac{M_0\beta_3}{2\beta_4}}\Big(\sqrt{\frac{3\beta_5}{2\beta_4}}\|u_h^0\|_1 + \frac{\sqrt{3}\beta_2}{\sqrt{\beta_1\beta_4}}\Big(\sum_{i=1}^{m} \frac{\Gamma(1-\alpha_i)t_n^{\alpha_i}}{b_i}\Big)^{1/2} \sup_{t\in[0,T]}\|f(t)\|\Big), \tag{4.8}$$

where h_0 is defined in Lemma 3.3 and $h_1 = \beta_4/\beta_3$.

Proof. Taking $v_h = u_h^n$ in (2.13), we can obtain

$$(\sum_{i=1}^{m} b_i D_N^{\alpha_i} u_h^n, \Pi_h^* u_h^n) + a(u_h^n, \Pi_h^* u_h^n) = (f^n, \Pi_h^* u_h^n). \tag{4.9}$$

Applying the definition of $D_N^{\alpha_i} u_h^n$ and Lemmas 3.1 and 3.3, we obtain

$$\sum_{i=1}^{m} \frac{b_i}{\Gamma(2-\alpha_i)} \sum_{k=0}^{n} \tilde{d}_{\alpha_i,k}^n (u_h^k, \Pi_h^* u_h^n) + \beta_4 \|u_h^n\|_1^2 \le \beta_2 \|f^n\| \cdot \|u_h^n\|. \tag{4.10}$$

Applying the Young inequality in (4.10), we have

$$\begin{aligned} &\sum_{i=1}^{m} \frac{b_i}{\Gamma(2-\alpha_i)} \tilde{d}_{\alpha_i,n}^n (u_h^n, \Pi_h^* u_h^n) + \beta_4 \|u_h^n\|_1^2 \\ \le &- \sum_{i=1}^{m} \frac{b_i}{\Gamma(2-\alpha_i)} \sum_{k=0}^{n-1} \tilde{d}_{\alpha_i,k}^n (u_h^k, \Pi_h^* u_h^n) + \frac{\beta_2^2}{2\beta_4} \|f^n\|^2 + \frac{\beta_4}{2} \|u_h^n\|^2. \end{aligned} \tag{4.11}$$

Noting that $\|u_h^n\| \le \|u_h^n\|_1$, we obtain

$$\begin{aligned} &\sum_{i=1}^{m} \frac{b_i}{\Gamma(2-\alpha_i)} \tilde{d}_{\alpha_i,n}^n (u_h^n, \Pi_h^* u_h^n) + \frac{\beta_4}{2} \|u_h^n\|_1^2 \\ \le &- \sum_{i=1}^{m} \frac{b_i}{\Gamma(2-\alpha_i)} \sum_{k=0}^{n-1} \tilde{d}_{\alpha_i,k}^n (u_h^k, \Pi_h^* u_h^n) + \frac{\beta_2^2}{2\beta_4} \|f^n\|^2. \end{aligned} \tag{4.12}$$

Applying Lemma 4.2, we have

$$(u_h^n, \Pi_h^* u_h^n) \le (u_h^0, \Pi_h^* u_h^0) + \frac{\beta_2^2}{2\beta_4} \sum_{i=1}^{m} \frac{\Gamma(1-\alpha_i) t_n^{\alpha_i}}{b_i} \sup_{t\in[0,T]} \|f(t)\|^2. \tag{4.13}$$

Thus, we apply Lemmas 3.1 and 3.3 to obtain (4.7).

Next, choosing $v_h = \sum\limits_{i=1}^{m} b_i D_N^{\alpha_i} u_h^n$ in (2.13), we have

$$(\sum_{i=1}^{m} b_i D_N^{\alpha_i} u_h^n, \Pi_h^* (\sum_{i=1}^{m} b_i D_N^{\alpha_i} u_h^n)) + a(u_h^n, \Pi_h^* (\sum_{i=1}^{m} b_i D_N^{\alpha_i} u_h^n)) = (f^n, \Pi_h^* (\sum_{i=1}^{m} b_i D_N^{\alpha_i} u_h^n)). \tag{4.14}$$

Invoking Lemma 4.1 in (4.14), we obtain

$$\begin{aligned} &(\sum_{i=1}^{m} b_i D_N^{\alpha_i} u_h^n, \Pi_h^* (\sum_{i=1}^{m} b_i D_N^{\alpha_i} u_h^n)) + \frac{1}{2} \sum_{i=1}^{m} \frac{b_i}{\Gamma(2-\alpha_i)} \tilde{d}_{\alpha_i,n}^n a(u_h^n, \Pi_h^* u_h^n) \\ &- \frac{1}{2} \sum_{i=1}^{m} \frac{b_i}{\Gamma(2-\alpha_i)} \sum_{k=0}^{n-1} \tilde{d}_{\alpha_i,k}^n a(u_h^n - u_h^k, \Pi_h^* (u_h^n - u_h^k)) \\ = &- \frac{1}{2} \sum_{i=1}^{m} \frac{b_i}{\Gamma(2-\alpha_i)} \sum_{k=0}^{n-1} \tilde{d}_{\alpha_i,k}^n a(u_h^k, \Pi_h^* u_h^k) + (f^n, \Pi_h^* (\sum_{i=1}^{m} b_i D_N^{\alpha_i} u_h^n)) \\ &- \frac{1}{2} \sum_{i=1}^{m} \frac{b_i}{\Gamma(2-\alpha_i)} \sum_{k=0}^{n-1} \tilde{d}_{\alpha_i,k}^n [a(u_h^n, \Pi_h^* u_h^k) - a(u_h^k, \Pi_h^* u_h^n)]. \end{aligned} \tag{4.15}$$

Noting that $\tilde{d}^n_{\alpha_i,k} < 0$ $(k = 0, 1, \cdots, n-1)$, and applying Lemma 3.3 and the Young inequality, we have

$$\begin{aligned}
&\beta_1\|\sum_{i=1}^{m} b_i D_N^{\alpha_i} u_h^n\|^2 + \frac{1}{2}\sum_{i=1}^{m}\frac{b_i}{\Gamma(2-\alpha_i)}\tilde{d}^n_{\alpha_i,n} a(u_h^n, \Pi_h^* u_h^n)\\
\leq &-\frac{1}{2}\sum_{i=1}^{m}\frac{b_i}{\Gamma(2-\alpha_i)}\sum_{k=0}^{n-1}\tilde{d}^n_{\alpha_i,k} a(u_h^k, \Pi_h^* u_h^k) + \frac{\beta_2^2}{2\beta_1}\|f^n\|^2 + \frac{\beta_1}{2}\|\sum_{i=1}^{m} b_i D_N^{\alpha_i} u_h^n\|^2\\
&-\frac{1}{2}\sum_{i=1}^{m}\frac{b_i}{\Gamma(2-\alpha_i)}\sum_{k=0}^{n-1}\tilde{d}^n_{\alpha_i,k}|a(u_h^n, \Pi_h^* u_h^k) - a(u_h^k, \Pi_h^* u_h^n)|.
\end{aligned} \tag{4.16}$$

From Lemmas 3.2 and 3.3, we have

$$|a(u_h^n, \Pi_h^* u_h^k) - a(u_h^k, \Pi_h^* u_h^n)| \leq \beta_3 h\|u_h^n\|_1\|u_h^k\|_1 \leq \frac{\beta_3}{2\beta_4} h\Big(a(u_h^n, \Pi_h^* u_h^n) + a(u_h^k, \Pi_h^* u_h^k)\Big). \tag{4.17}$$

Substituting (4.17) into (4.16), we obtain

$$\begin{aligned}
&\frac{\beta_1}{2}\|\sum_{i=1}^{m} b_i D_N^{\alpha_i} u_h^n\|^2 + \frac{1}{2}\sum_{i=1}^{m}\frac{b_i}{\Gamma(2-\alpha_i)}\tilde{d}^n_{\alpha_i,n} a(u_h^n, \Pi_h^* u_h^n)\\
\leq &-\frac{1}{2}\sum_{i=1}^{m}\frac{b_i}{\Gamma(2-\alpha_i)}\sum_{k=0}^{n-1}\tilde{d}^n_{\alpha_i,k} a(u_h^k, \Pi_h^* u_h^k) + \frac{\beta_2^2}{2\beta_1}\|f^n\|^2\\
&-\frac{1}{2}\sum_{i=1}^{m}\frac{b_i}{\Gamma(2-\alpha_i)}\sum_{k=0}^{n-1}\tilde{d}^n_{\alpha_i,k}\frac{\beta_3}{2\beta_4} h\Big(a(u_h^n, \Pi_h^* u_h^n) + a(u_h^k, \Pi_h^* u_h^k)\Big).
\end{aligned} \tag{4.18}$$

Noting that $\sum\limits_{k=0}^{n-1}\tilde{d}^n_{\alpha_i,k} = -\tilde{d}^n_{\alpha_i,n}$, we have

$$\begin{aligned}
&\frac{\beta_1}{2}\|\sum_{i=1}^{m} b_i D_N^{\alpha_i} u_h^n\|^2 + \frac{1}{2}\sum_{i=1}^{m}\frac{b_i}{\Gamma(2-\alpha_i)}\tilde{d}^n_{\alpha_i,n}\Big(1 - \frac{\beta_3}{2\beta_4} h\Big)a(u_h^n, \Pi_h^* u_h^n)\\
\leq &-\frac{1}{2}\sum_{i=1}^{m}\frac{b_i}{\Gamma(2-\alpha_i)}\sum_{k=0}^{n-1}\tilde{d}^n_{\alpha_i,k}\Big(1 + \frac{\beta_3}{2\beta_4} h\Big)a(u_h^k, \Pi_h^* u_h^k) + \frac{\beta_2^2}{2\beta_1}\|f^n\|^2.
\end{aligned} \tag{4.19}$$

Setting $h_1 = \beta_4/\beta_3$, when $h \leq h_1$, we have $(1 - \frac{\beta_3}{2\beta_4} h) \geq \frac{1}{2}$ and

$$\sum_{i=1}^{m}\frac{b_i}{\Gamma(2-\alpha_i)}\tilde{d}^n_{\alpha_i,n} a(u_h^n, \Pi_h^* u_h^n) \leq -\left(\frac{1 + \frac{\beta_3}{2\beta_4} h}{1 - \frac{\beta_3}{2\beta_4} h}\right)\sum_{i=1}^{m}\frac{b_i}{\Gamma(2-\alpha_i)}\sum_{k=0}^{n-1}\tilde{d}^n_{\alpha_i,k} a(u_h^k, \Pi_h^* u_h^k) + \frac{2\beta_2^2}{\beta_1}\|f^n\|^2. \tag{4.20}$$

Applying Lemma 4.2, we have

$$a(u_h^n, \Pi_h^* u_h^n) \leq \left(\frac{1 + \frac{\beta_3}{2\beta_4} h}{1 - \frac{\beta_3}{2\beta_4} h}\right)^n \Big(a(u_h^0, \Pi_h^* u_h^0) + \frac{2\beta_2^2}{\beta_1}\sum_{i=1}^{m}\frac{\Gamma(1-\alpha_i) t_n^{\alpha_i}}{b_i}\sup_{t\in[0,T]}\|f(t)\|^2\Big). \tag{4.21}$$

Let $M_0 > 0$ be a constant. Choosing N and h to satisfy $h \le M_0/N$, and applying Lemma 3.3, we have

$$\beta_4\|u_h^n\|_1^2 \le \left(\frac{1+\frac{M_0\beta_3}{2\beta_4 N}}{1-\frac{M_0\beta_3}{2\beta_4 N}}\right)^N \Big(\beta_5\|u_h^0\|_1^2 + \frac{2\beta_2^2}{\beta_1}\sum_{i=1}^{m}\frac{\Gamma(1-\alpha_i)t_n^{\alpha_i}}{b_i}\sup_{t\in[0,T]}\|f(t)\|^2\Big). \tag{4.22}$$

Note that

$$\lim_{N\to\infty}\left(\frac{1+\frac{M_0\beta_3}{2\beta_4 N}}{1-\frac{M_0\beta_3}{2\beta_4 N}}\right)^N = e^{\frac{M_0\beta_3}{\beta_4}}, \tag{4.23}$$

then there exists an integer $N_0 > 0$ such that if $N \ge N_0$, then

$$\left(\frac{1+\frac{M_0\beta_3}{2\beta_4 N}}{1-\frac{M_0\beta_3}{2\beta_4 N}}\right)^N \le \frac{3}{2}e^{\frac{M_0\beta_3}{\beta_4}}. \tag{4.24}$$

Finally, substituting (4.24) into (4.22) finalizes the proof. □

Remark 4.1. *According to Theorem 4.1, it can be seen that the fully discrete solution u_h^n in the $L^2(\Omega)$ norm is unconditionally stable, and that in the $H^1(\Omega)$ norm is stable if the required conditions can be met due to the fact that $a(\cdot, \Pi_h^*\cdot)$ may not necessarily possess symmetry. From [46], if $\mathcal{A}(\boldsymbol{x})$ is a constant matrix, satisfies symmetry, and is positive definite, it can be derived that $a(\cdot, \Pi_h^*\cdot)$ possesses symmetry, and u_h^n in the $H^1(\Omega)$ norm is also unconditionally stable.*

5. Error estimates

In order to obtain the error estimates for the fully discrete FVE scheme (2.13), we first give the estimates of the truncation error $R_{\alpha_i}^n$.

Lemma 5.1. *[21, 22] There exists a constant $C > 0$ independent of N and h such that*

$$\|R_{\alpha_i}^n\| \le CN^{-(2-\alpha_i)},\ 1 \le i \le m, \tag{5.1}$$

$$\|\sum_{i=1}^{m} b_i R_{\alpha_i}^n\| \le CN^{-(2-\alpha_1)}, \tag{5.2}$$

where the positive integer N is the time mesh parameter defined in Section 2.

Next, we introduce an elliptic projection operator $P_h : H_0^1(\Omega)\cap H^2(\Omega) \to U_h$ as follows:

$$a(u - P_h u, \Pi_h^* v_h) = 0,\ \forall v_h \in U_h. \tag{5.3}$$

Then, the following estimates of the projection operator P_h can be obtained.

Lemma 5.2. *[32, 47] There exists a constant $C > 0$ independent of h such that*

$$\|u - P_h u\|_1 \le Ch|u|_2,\ \forall u \in H_0^1(\Omega)\cap H^2(\Omega), \tag{5.4}$$

$$\|u - P_h u\| \le Ch^2\|u\|_{3,p},\ \forall u \in H_0^1(\Omega)\cap W^{3,p}(\Omega),\ p > 1. \tag{5.5}$$

Now, we derive the following error estimates for the fully discrete FVE scheme (2.13).

Theorem 5.1. *Let u be the solution of primal model* (1.1)*, and u_h^n be the solution of the FVE scheme* (2.13)*. Assume that $u_h^0 = P_h u_0$, then there exists a constant $C > 0$ independent of N and h such that*

$$\max_{1\le n\le N} \|u(t_n) - u_h^n\| \le C(N^{-(2-\alpha_1)} + h^2). \tag{5.6}$$

Moreover, there exists a constant $C > 0$ independent of N and h such that if $h \le M_0/N \le M_0/N_0$ and $h \le \min\{h_0, h_1\}$, then

$$\max_{1\le n\le N} \|u(t_n) - u_h^n\|_1 \le C\Big(h + e^{\frac{M_0\beta_3}{2\beta_4}}(N^{-(2-\alpha_1)} + h^2)\Big), \tag{5.7}$$

where h_0 is defined in Lemma 3.3, and h_1, M_0, and N_0 are defined in Theorem 4.1.

Proof. Let $u(t_n) - u_h^n = \rho^n + \theta^n$, where $\rho^n = u(t_n) - P_h u(t_n)$, $\theta^n = P_h u(t_n) - u_h^n$, and P_h is the elliptic projection operator. From Lemma 5.2, we only need to estimate θ^n and obtain the error equation for θ^n as follows:

$$(\sum_{i=1}^{m} b_i D_N^{\alpha_i}\theta^n, \Pi_h^* v_h) + a(\theta^n, \Pi_h^* v_h) = -(\sum_{i=1}^{m} b_i D_N^{\alpha_i}\rho^n, \Pi_h^* v_h) - (\sum_{i=1}^{m} b_i R_{\alpha_i}^n, \Pi_h^* v_h),\ \forall v_h \in U_h. \tag{5.8}$$

Taking $v_h = \theta^n$ in (5.8), applying Lemma 3.3 and the definition of $D_N^{\alpha_i}\theta^n$, we obtain

$$\begin{aligned} &\sum_{i=1}^{m} \frac{b_i}{\Gamma(2-\alpha_i)} \tilde{d}_{\alpha_i,n}^n(\theta^n, \Pi_h^*\theta^n) + \beta_4\|\theta^n\|_1^2 \\ \le &-\sum_{i=1}^{m} \frac{b_i}{\Gamma(2-\alpha_i)} \sum_{k=0}^{n-1} \tilde{d}_{\alpha_i,k}^n(\theta^k, \Pi_h^*\theta^n) - (\sum_{i=1}^{m} b_i D_N^{\alpha_i}\rho^n, \Pi_h^*\theta^n) - (\sum_{i=1}^{m} b_i R_{\alpha_i}^n, \Pi_h^*\theta^n). \end{aligned} \tag{5.9}$$

Applying the Young inequality in (5.9), we obtain

$$\begin{aligned} &\sum_{i=1}^{m} \frac{b_i}{\Gamma(2-\alpha_i)} \tilde{d}_{\alpha_i,n}^n(\theta^n, \Pi_h^*\theta^n) + \beta_4\|\theta^n\|_1^2 \\ \le &-\sum_{i=1}^{m} \frac{b_i}{\Gamma(2-\alpha_i)} \sum_{k=0}^{n-1} \tilde{d}_{\alpha_i,k}^n(\theta^k, \Pi_h^*\theta^n) + C(\|\sum_{i=1}^{m} b_i D_N^{\alpha_i}\rho^n\|^2 + \|\sum_{i=1}^{m} b_i R_{\alpha_i}^n\|^2) + \frac{\beta_4}{2}\|\theta^n\|^2. \end{aligned} \tag{5.10}$$

From [39], we know that

$$\|D_N^{\alpha_i}\rho^n\|^2 \le CT^{2-2\alpha_i}h^4\|u_t\|_{L^\infty(W^{3,p})}^2,\ p > 1. \tag{5.11}$$

Applying Lemma 5.1, we obtain

$$\begin{aligned} &\sum_{i=1}^{m} \frac{b_i}{\Gamma(2-\alpha_i)} \tilde{d}_{\alpha_i,n}^n(\theta^n, \Pi_h^*\theta^n) + \frac{\beta_4}{2}\|\theta^n\|_1^2 \\ \le &-\sum_{i=1}^{m} \frac{b_i}{\Gamma(2-\alpha_i)} \sum_{k=0}^{n-1} \tilde{d}_{\alpha_i,k}^n(\theta^k, \Pi_h^*\theta^n) + C(N^{-2(2-\alpha_1)} + h^4). \end{aligned} \tag{5.12}$$

Noting that $\theta^0 = 0$ and applying Lemmas 3.1 and 4.2, we obtain

$$\beta_1\|\theta^n\|^2 \le (\theta^n, \Pi_h^*\theta^n) \le C(N^{-2(2-\alpha_1)} + h^4). \tag{5.13}$$

In order to estimate $\|u - u_h\|_1$, we take $v_h = \sum\limits_{i=1}^{m} b_i D_N^{\alpha_i}\theta^n$ in (5.8), and obtain

$$\begin{aligned}
&(\sum_{i=1}^{m} b_i D_N^{\alpha_i}\theta^n, \Pi_h^*(\sum_{i=1}^{m} b_i D_N^{\alpha_i}\theta^n)) + a(\theta^n, \Pi_h^*(\sum_{i=1}^{m} b_i D_N^{\alpha_i}\theta^n))\\
&= -(\sum_{i=1}^{m} b_i D_N^{\alpha_i}\rho^n, \Pi_h^*(\sum_{i=1}^{m} b_i D_N^{\alpha_i}\theta^n)) - (\sum_{i=1}^{m} b_i R_{\alpha_i}^n, \Pi_h^*(\sum_{i=1}^{m} b_i D_N^{\alpha_i}\theta^n)).
\end{aligned} \tag{5.14}$$

Applying Lemma 4.1, we have

$$\begin{aligned}
&(\sum_{i=1}^{m} b_i D_N^{\alpha_i}\theta^n, \Pi_h^*(\sum_{i=1}^{m} b_i D_N^{\alpha_i}\theta^n)) + \frac{1}{2}\sum_{i=1}^{m}\frac{b_i}{\Gamma(2-\alpha_i)}\tilde{d}_{\alpha_i,n}^n a(\theta^n, \Pi_h^*\theta^n)\\
&- \frac{1}{2}\sum_{i=1}^{m}\frac{b_i}{\Gamma(2-\alpha_i)}\sum_{k=0}^{n-1}\tilde{d}_{\alpha_i,k}^n a(\theta^n - \theta^k, \Pi_h^*(\theta^n - \theta^k))\\
&= -\frac{1}{2}\sum_{i=1}^{m}\frac{b_i}{\Gamma(2-\alpha_i)}\sum_{k=0}^{n-1}\tilde{d}_{\alpha_i,k}^n a(\theta^k, \Pi_h^*\theta^k) - (\sum_{i=1}^{m} b_i D_N^{\alpha_i}\rho^n, \Pi_h^*(\sum_{i=1}^{m} b_i D_N^{\alpha_i}\theta^n))\\
&- \frac{1}{2}\sum_{i=1}^{m}\frac{b_i}{\Gamma(2-\alpha_i)}\sum_{k=0}^{n-1}\tilde{d}_{\alpha_i,k}^n [a(\theta^n, \Pi_h^*\theta^k) - a(\theta^k, \Pi_h^*\theta^n)] - (\sum_{i=1}^{m} b_i R_{\alpha_i}^n, \Pi_h^*(\sum_{i=1}^{m} b_i D_N^{\alpha_i}\theta^n)).
\end{aligned} \tag{5.15}$$

Noting that $\tilde{d}_{\alpha_i,k}^n < 0$ ($k = 0, 1, \cdots, n-1$), and invoking the Young inequality, we have

$$\begin{aligned}
&\beta_1\|\sum_{i=1}^{m} b_i D_N^{\alpha_i}\theta^n\|^2 + \frac{1}{2}\sum_{i=1}^{m}\frac{b_i}{\Gamma(2-\alpha_i)}\tilde{d}_{\alpha_i,n}^n a(\theta^n, \Pi_h^*\theta^n)\\
&\le -\frac{1}{2}\sum_{i=1}^{m}\frac{b_i}{\Gamma(2-\alpha_i)}\sum_{k=0}^{n-1}\tilde{d}_{\alpha_i,k}^n a(\theta^k, \Pi_h^*\theta^k) + C\Big(\|\sum_{i=1}^{m} b_i D_N^{\alpha_i}\rho^n\|^2 + \|\sum_{i=1}^{m} b_i R_{\alpha_i}^n\|^2\Big)\\
&- \frac{1}{2}\sum_{i=1}^{m}\frac{b_i}{\Gamma(2-\alpha_i)}\sum_{k=0}^{n-1}\tilde{d}_{\alpha_i,k}^n |a(\theta^n, \Pi_h^*\theta^k) - a(\theta^k, \Pi_h^*\theta^n)| + \frac{\beta_1}{2}\|\sum_{i=1}^{m} b_i D_N^{\alpha_i}\theta^n\|^2.
\end{aligned} \tag{5.16}$$

From Lemmas 3.2 and 3.3, we have

$$|a(\theta^n, \Pi_h^*\theta^k) - a(\theta^k, \Pi_h^*\theta^n)| \le \beta_3 h\|\theta^n\|_1\|\theta^k\|_1 \le \frac{\beta_3}{2\beta_4}h[a(\theta^n, \Pi_h^*\theta^n) + a(\theta^k, \Pi_h^*\theta^k)]. \tag{5.17}$$

Substituting (5.11) and (5.17) into (5.16), and noting that $\sum\limits_{k=0}^{n-1}\tilde{d}_{\alpha_i,k}^n = -\tilde{d}_{\alpha_i,n}^n$, we have

$$\begin{aligned}
&\frac{\beta_1}{2}\|\sum_{i=1}^{m} b_i D_N^{\alpha_i}\theta^n\|^2 + \frac{1}{2}\sum_{i=1}^{m}\frac{b_i}{\Gamma(2-\alpha_i)}\tilde{d}_{\alpha_i,n}^n\Big(1 - \frac{\beta_3}{2\beta_4}h\Big)a(\theta^n, \Pi_h^*\theta^n)\\
&\le -\frac{1}{2}\sum_{i=1}^{m}\frac{b_i}{\Gamma(2-\alpha_i)}\sum_{k=0}^{n-1}\tilde{d}_{\alpha_i,k}^n\Big(1 + \frac{\beta_3}{2\beta_4}h\Big)a(\theta^k, \Pi_h^*\theta^k) + C(h^4 + N^{-2(2-\alpha_1)}).
\end{aligned} \tag{5.18}$$

Analogous to the process of (4.19) and (4.20), when $h \le h_1$, we have $(1 - \frac{\beta_3}{2\beta_4}h) \ge \frac{1}{2}$, and

$$\begin{aligned} &\sum_{i=1}^{m} \frac{b_i}{\Gamma(2-\alpha_i)} \tilde{d}^n_{\alpha_i,n} a(\theta^n, \Pi_h^* \theta^n) \\ &\le -\left(\frac{1+\frac{\beta_3}{2\beta_4}h}{1-\frac{\beta_3}{2\beta_4}h}\right) \sum_{i=1}^{m} \frac{b_i}{\Gamma(2-\alpha_i)} \sum_{k=0}^{n-1} \tilde{d}^n_{\alpha_i,k} a(\theta^k, \Pi_h^* \theta^k) + C(h^4 + N^{-2(2-\alpha_1)}). \end{aligned} \tag{5.19}$$

Applying Lemma 4.2 and noting that $\theta^0 = 0$, we have

$$a(\theta^n, \Pi_h^* \theta^n) \le C\left(\frac{1+\frac{\beta_3}{2\beta_4}h}{1-\frac{\beta_3}{2\beta_4}h}\right)^n (h^4 + N^{-2(2-\alpha_1)}). \tag{5.20}$$

Choosing N and h to satisfy $h \le M_0/N$ in (5.19), where M_0 is defined in Theorem 4.1, we have

$$a(\theta^n, \Pi_h^* \theta^n) \le C\left(\frac{1+\frac{M_0\beta_3}{2\beta_4 N}}{1-\frac{M_0\beta_3}{2\beta_4 N}}\right)^N (h^4 + N^{-2(2-\alpha_1)}). \tag{5.21}$$

From (4.23) and (4.24), it follows that if $N \ge N_0$, where N_0 is defined in Theorem 4.1, then,

$$a(\theta^n, \Pi_h^* \theta^n) \le C e^{\frac{M_0\beta_3}{\beta_4}} (h^4 + N^{-2(2-\alpha_1)}). \tag{5.22}$$

Thus, we utilize Lemmas 3.3 and 5.2 to finalize the proof. □

6. Numerical examples

In this section, we will give three examples to examine the feasibility and effectiveness of the proposed FVE scheme by using the Matlab software. Moreover, we will calculate the errors by using the discrete norms $\|u-u_h\|_{\tilde{L}^\infty(L^2(\Omega))} = \max_{1\le n\le N} \|u(t_n)-u_h^n\|$ and $\|u-u_h\|_{\tilde{L}^\infty(H^1(\Omega))} = \max_{1\le n\le N} \|u(t_n)-u_h^n\|_1$, which are referred to as the discrete $L^\infty(L^2(\Omega))$ norm and discrete $L^\infty(H^1(\Omega))$ norm, respectively.

Example 6.1. Consider the following two-term TFRD model

$$\begin{cases} \{D_t^{\alpha_1} + D_t^{\alpha_2}\}u(\boldsymbol{x},t) - \mathrm{div}(\mathcal{A}(\boldsymbol{x})\nabla u(\boldsymbol{x},t)) + q(\boldsymbol{x})u(\boldsymbol{x},t) = f(\boldsymbol{x},t), & (\boldsymbol{x},t) \in \Omega \times J, \\ u(\boldsymbol{x},t) = 0, & (\boldsymbol{x},t) \in \partial\Omega \times J, \\ u(\boldsymbol{x},0) = u_0(\boldsymbol{x}), & \boldsymbol{x} \in \Omega, \end{cases} \tag{6.1}$$

where $\Omega = (0,1)^2$, $J = (0,1]$, $q(\boldsymbol{x}) = 2 + x_1^2 + x_2^2$, and

$$\mathcal{A}(\boldsymbol{x}) = \begin{bmatrix} 1 + 2x_1^2 + 2x_2^2, & x_1^2 + x_2^2 \\ x_1^2 + x_2^2, & 1 + x_1^2 + x_2^2 \end{bmatrix},$$

where $\boldsymbol{x} = (x_1, x_2) \in \Omega$. We take the exact solution $u(\boldsymbol{x},t)$ as follows:

$$u(\boldsymbol{x},t) = t^{2.5+\alpha_1+\alpha_2} \sin(2\pi x_1) \sin(2\pi x_2),$$

and easily obtain the source function $f(\boldsymbol{x},t)$ and initial data $u_0(\boldsymbol{x})$.

According to Theorem 5.1, we know that convergence accuracy is only related to the maximum fractional parameter α_1. Now, we choose fractional parameters $\alpha_1 = 0.8, 0.6, 0.4$, and $\alpha_2 = 0.1, 0.3$ in (6.1), and give numerical results and convergence rates in Tables 1–8 for this example. In Tables 1–3, we perform numerical simulation calculations by taking $N = 10, 20, 40, 50$ and $h = \sqrt{2}/N$, and observe that the convergence rates for u in the discrete $L^\infty(L^2(\Omega))$ and $L^\infty(H^1(\Omega))$ norms are close to 2 and 1, respectively. Next, we will abandon condition $h \leq M_0/N$ for numerical experiments, give numerical results in Tables 4–6 by maintaining $N = 1000$ and taking $h = \sqrt{2}/10$, $\sqrt{2}/20$, $\sqrt{2}/25$, $\sqrt{2}/40$, and observe that the convergence rates for u in the discrete $L^\infty(L^2(\Omega))$ norm with respect to the spatial direction are close to 2 and in the discrete $L^\infty(H^1(\Omega))$ norm are close to 1. This indicates that condition $h \leq M_0/N$ does not have any impact on the actual experiments. Finally, we will examine the convergence rates with respect to the temporal direction. Noting that $\|u-u_h\|_{L^\infty(L^2(\Omega))} = O(h^2+N^{-(2-\alpha_1)})$, we take $N = 20, 40, 100, 160$ and $h \approx \sqrt{2}N^{-(1-\alpha_1/2)}$, and give numerical results in Table 7, which can be seen that the convergence rates for u in the discrete $L^\infty(L^2(\Omega))$ norm with respect to the temporal direction are close to $2 - \alpha_1$. Furthermore, noting that $\|u - u_h\|_{L^\infty(H^1(\Omega))} = O(h + N^{-(2-\alpha_1)})$, we take $N = 5, 8, 10, 14$ and $h \approx \sqrt{2}N^{-(2-\alpha_1)}$, and give numerical results in Table 8, which can be seen that the convergence rates for u in the discrete $L^\infty(H^1(\Omega))$ norm with respect to the temporal direction are also close to $2 - \alpha_1$. The convergence rates obtained from numerical experiments above are in agreement with the theoretical analysis results.

Table 1. Error behaviors with $h = \sqrt{2}/N$ and $\alpha_1 = 0.8$ in Example 6.1.

α_2	(h, N)	$\|u - u_h\|_{\tilde{L}^\infty(L^2)}$	Rates	$\|u - u_h\|_{\tilde{L}^\infty(H^1)}$	Rates
0.1	$(\sqrt{2}/10, 10)$	3.3318E-02		1.3248E+00	
	$(\sqrt{2}/20, 20)$	8.0234E-03	2.0540	6.7065E-01	0.9821
	$(\sqrt{2}/40, 40)$	1.9363E-03	2.0509	3.3668E-01	0.9942
	$(\sqrt{2}/50, 50)$	1.2231E-03	2.0587	2.6951E-01	0.9972
0.3	$(\sqrt{2}/10, 10)$	3.3137E-02		1.3250E+00	
	$(\sqrt{2}/20, 20)$	7.9536E-03	2.0588	6.7069E-01	0.9823
	$(\sqrt{2}/40, 40)$	1.9108E-03	2.0575	3.3669E-01	0.9943
	$(\sqrt{2}/50, 50)$	1.2046E-03	2.0675	2.6952E-01	0.9972

Table 2. Error behaviors with $h = \sqrt{2}/N$ and $\alpha_1 = 0.6$ in Example 6.1.

α_2	(h, N)	$\|u - u_h\|_{\tilde{L}^\infty(L^2)}$	Rates	$\|u - u_h\|_{\tilde{L}^\infty(H^1)}$	Rates
0.1	$(\sqrt{2}/10, 10)$	3.3705E-02		1.3243E+00	
	$(\sqrt{2}/20, 20)$	8.2081E-03	2.0379	6.7053E-01	0.9819
	$(\sqrt{2}/40, 40)$	2.0183E-03	2.0239	3.3665E-01	0.9941
	$(\sqrt{2}/50, 50)$	1.2860E-03	2.0197	2.6950E-01	0.9971
0.3	$(\sqrt{2}/10, 10)$	3.3574E-02		1.3245E+00	
	$(\sqrt{2}/20, 20)$	8.1626E-03	2.0402	6.7056E-01	0.9820
	$(\sqrt{2}/40, 40)$	2.0037E-03	2.0264	3.3665E-01	0.9941
	$(\sqrt{2}/50, 50)$	1.2759E-03	2.0226	2.6950E-01	0.9971

Table 3. Error behaviors with $h = \sqrt{2}/N$ and $\alpha_1 = 0.4$ in Example 6.1.

α_2	(h, N)	$\|u - u_h\|_{\tilde{L}^\infty(L^2)}$	Rates	$\|u - u_h\|_{\tilde{L}^\infty(H^1)}$	Rates
0.1	$(\sqrt{2}/10, 10)$	3.3902E-02		1.3241E+00	
	$(\sqrt{2}/20, 20)$	8.2861E-03	2.0326	6.7049E-01	0.9817
	$(\sqrt{2}/40, 40)$	2.0474E-03	2.0169	3.3664E-01	0.9940
	$(\sqrt{2}/50, 50)$	1.3072E-03	2.0108	2.6949E-01	0.9970
0.3	$(\sqrt{2}/10, 10)$	3.3798E-02		1.3242E+00	
	$(\sqrt{2}/20, 20)$	8.2523E-03	2.0341	6.7051E-01	0.9818
	$(\sqrt{2}/40, 40)$	2.0372E-03	2.0182	3.3664E-01	0.9940
	$(\sqrt{2}/50, 50)$	1.3003E-03	2.0121	2.6949E-01	0.9971

Table 4. Error behaviors with $N = 1000$ and $\alpha_1 = 0.8$ in Example 6.1.

α_2	h	$\|u - u_h\|_{\tilde{L}^\infty(L^2)}$	Rates	$\|u - u_h\|_{\tilde{L}^\infty(H^1)}$	Rates
0.1	$\sqrt{2}/10$	3.3776E-02		1.3242E+00	
	$\sqrt{2}/20$	8.2574E-03	2.0322	6.7050E-01	0.9818
	$\sqrt{2}/25$	5.2645E-03	2.0172	5.3734E-01	0.9921
	$\sqrt{2}/40$	2.0409E-03	2.0162	3.3664E-01	0.9949
0.3	$\sqrt{2}/10$	3.3695E-02		1.3243E+00	
	$\sqrt{2}/20$	8.2347E-03	2.0327	6.7051E-01	0.9819
	$\sqrt{2}/25$	5.2498E-03	2.0174	5.3735E-01	0.9922
	$\sqrt{2}/40$	2.0348E-03	2.0165	3.3664E-01	0.9949

Table 5. Error behaviors with $N = 1000$ and $\alpha_1 = 0.6$ in Example 6.1.

α_2	h	$\|u - u_h\|_{\tilde{L}^\infty(L^2)}$	Rates	$\|u - u_h\|_{\tilde{L}^\infty(H^1)}$	Rates
0.1	$\sqrt{2}/10$	3.3886E-02		1.3241E+00	
	$\sqrt{2}/20$	8.2894E-03	2.0313	6.7048E-01	0.9817
	$\sqrt{2}/25$	5.2859E-03	2.0164	5.3733E-01	0.9921
	$\sqrt{2}/40$	2.0505E-03	2.0148	3.3664E-01	0.9949
0.3	$\sqrt{2}/10$	3.3815E-02		1.3241E+00	
	$\sqrt{2}/20$	8.2698E-03	2.0318	6.7049E-01	0.9818
	$\sqrt{2}/25$	5.2732E-03	2.0165	5.3734E-01	0.9921
	$\sqrt{2}/40$	2.0454E-03	2.0149	3.3664E-01	0.9949

Table 6. Error behaviors with $N = 1000$ and $\alpha_1 = 0.4$ in Example 6.1.

α_2	h	$\|u - u_h\|_{\tilde{L}^\infty(L^2)}$	Rates	$\|u - u_h\|_{\tilde{L}^\infty(H^1)}$	Rates
0.1	$\sqrt{2}/10$	3.3968E-02		1.3240E+00	
	$\sqrt{2}/20$	8.3123E-03	2.0308	6.7047E-01	0.9817
	$\sqrt{2}/25$	5.3008E-03	2.0161	5.3733E-01	0.9921
	$\sqrt{2}/40$	2.0565E-03	2.0145	3.3664E-01	0.9949
0.3	$\sqrt{2}/10$	3.3905E-02		1.3241E+00	
	$\sqrt{2}/20$	8.2949E-03	2.0312	6.7048E-01	0.9817
	$\sqrt{2}/25$	5.2895E-03	2.0162	5.3733E-01	0.9921
	$\sqrt{2}/40$	2.0521E-03	2.0146	3.3664E-01	0.9949

Table 7. Error $\|u - u_h\|_{\tilde{L}^\infty(L^2)}$ with $h \approx \sqrt{2}N^{-(1-\alpha_1/2)}$ in Example 6.1.

(α_1, α_2)	N	20	40	100	160
(0.8,0.1)	Error	9.5444E-02	4.2273E-02	1.2944E-02	7.4718E-03
	Rates		1.1749	1.2917	1.1691
(0.8,0.3)	Error	9.5249E-02	4.2160E-02	1.2903E-02	7.4480E-03
	Rates		1.1758	1.2922	1.1692
(0.6,0.1)	Error	5.3384E-02	1.9902E-02	5.2773E-03	2.6785E-03
	Rates		1.4235	1.4487	1.4428
(0.6,0.3)	Error	5.3263E-02	1.9849E-02	5.2622E-03	2.6708E-03
	Rates		1.4241	1.4489	1.4429
(0.4,0.1)	Error	2.8117E-02	9.2248E-03	2.0544E-03	9.7424E-04
	Rates		1.6079	1.6391	1.5874
(0.4,0.3)	Error	2.8049E-02	9.2001E-03	2.0487E-03	9.7151E-04
	Rates		1.6082	1.6392	1.5874

Table 8. Error $\|u - u_h\|_{\tilde{L}^\infty(H^1)}$ with $h \approx \sqrt{2}N^{-(1-\alpha_1)}$ in Example 6.1.

(α_1, α_2)	N	5	8	10	14
(0.8,0.1)	Error	1.8594E+00	1.1095E+00	8.3636E-01	5.5981E-01
	Rates		1.0985	1.2666	1.1931
(0.8,0.3)	Error	1.8600E+00	1.1098E+00	8.3649E-01	5.5987E-01
	Rates		1.0988	1.2668	1.1933
(0.6,0.1)	Error	1.4652E+00	7.4434E-01	5.3744E-01	3.3668E-01
	Rates		1.4409	1.4595	1.3899
(0.6,0.3)	Error	1.4655E+00	7.4443E-01	5.3749E-01	3.3670E-01
	Rates		1.4411	1.4597	1.3900
(0.4,0.1)	Error	1.0251E+00	4.8018E-01	3.3666E-01	1.9829E-01
	Rates		1.6135	1.5913	1.5732
(0.4,0.3)	Error	1.0252E+00	4.8022E-01	3.3668E-01	1.9830E-01
	Rates		1.6137	1.5914	1.5733

Example 6.2. Consider the following three-term TFRD model

$$\begin{cases} \{D_t^{\alpha_1} + D_t^{\alpha_2} + D_t^{\alpha_3}\}u(\boldsymbol{x},t) - \mathrm{div}(\mathcal{A}(\boldsymbol{x})\nabla u(\boldsymbol{x},t)) + q(\boldsymbol{x})u(\boldsymbol{x},t) = f(\boldsymbol{x},t), & (\boldsymbol{x},t) \in \Omega \times J, \\ u(\boldsymbol{x},t) = 0, & (\boldsymbol{x},t) \in \partial\Omega \times J, \\ u(\boldsymbol{x},0) = u_0(\boldsymbol{x}), & \boldsymbol{x} \in \Omega, \end{cases} \tag{6.2}$$

where Ω, J, $q(\boldsymbol{x})$, and $\mathcal{A}(\boldsymbol{x})$ are same as in Example 6.1. Here, we take the exact solution $u(\boldsymbol{x},t) = t^{2.5+\alpha_1+\alpha_2+\alpha_3}\sin(2\pi x_1)\sin(2\pi x_2)$, and easily obtain the source function $f(\boldsymbol{x},t)$ and initial data $u_0(\boldsymbol{x})$.

Different from Example 6.1, note that (6.2) includes three fractional derivative terms in this example, hence, we conducted numerical simulations by specifically taking the fractional parameters $\alpha_1 = 0.8, 0.6, 0.4$, $(\alpha_2, \alpha_3) = (0.3, 0.1), (0.3, 0.2)$. By taking $N = 10, 20, 40, 50$, and the corresponding $h = \sqrt{2}/N$, we display the numerical results in Tables 9–11, and observe that the convergence rates for u in the discrete $L^\infty(L^2(\Omega))$ norm are close to 2 and in the discrete $L^\infty(H^1(\Omega))$ norm are close to 1. In Tables 12–14, we also abandon condition $h \le M_0/N$ for numerical experiments, test the convergence rates with respect to the spatial direction by fixing $N = 1000$ and taking $h = \sqrt{2}/10, \sqrt{2}/20, \sqrt{2}/25, \sqrt{2}/40$, and observe that the convergence rates for u in the discrete $L^\infty(L^2(\Omega))$ and $L^\infty(H^1(\Omega))$ norms with respect to the spatial direction are close to 2 and 1, respectively. Finally, we use the same method as Example 6.1 to examine the convergence rates with respect to the temporal direction, and give the numerical results in Tables 15 and 16, which indicate that the convergence rates for u in the discrete $L^\infty(L^2(\Omega))$ and $L^\infty(H^1(\Omega))$ norms are also close to $2 - \alpha_1$.

Table 9. Error behaviors with $h = \sqrt{2}/N$ and $\alpha_1 = 0.8$ in Example 6.2.

(α_2, α_3)	(h, N)	$\|u - u_h\|_{\tilde{L}^\infty(L^2)}$	Rates	$\|u - u_h\|_{\tilde{L}^\infty(H^1)}$	Rates
(0.3,0.1)	$(\sqrt{2}/10, 10)$	3.2906E-02		1.3253E+00	
	$(\sqrt{2}/20, 20)$	7.8824E-03	2.0616	6.7074E-01	0.9825
	$(\sqrt{2}/40, 40)$	1.8898E-03	2.0604	3.3669E-01	0.9943
	$(\sqrt{2}/50, 50)$	1.1904E-03	2.0712	2.6952E-01	0.9972
(0.3,0.2)	$(\sqrt{2}/10, 10)$	3.2815E-02		1.3254E+00	
	$(\sqrt{2}/20, 20)$	7.8473E-03	2.0641	6.7076E-01	0.9825
	$(\sqrt{2}/40, 40)$	1.8770E-03	2.0638	3.3670E-01	0.9943
	$(\sqrt{2}/50, 50)$	1.1812E-03	2.0757	2.6953E-01	0.9972

Table 10. Error behaviors with $h = \sqrt{2}/N$ and $\alpha_1 = 0.6$ in Example 6.2.

(α_2, α_3)	(h, N)	$\|u - u_h\|_{\tilde{L}^\infty(L^2)}$	Rates	$\|u - u_h\|_{\tilde{L}^\infty(H^1)}$	Rates
(0.3,0.1)	$(\sqrt{2}/10, 10)$	3.3359E-02		1.3247E+00	
	$(\sqrt{2}/20, 20)$	8.1000E-03	2.0421	6.7059E-01	0.9821
	$(\sqrt{2}/40, 40)$	1.9867E-03	2.0275	3.3666E-01	0.9942
	$(\sqrt{2}/50, 50)$	1.2648E-03	2.0237	2.6950E-01	0.9971
(0.3,0.2)	$(\sqrt{2}/10, 10)$	3.3292E-02		1.3248E+00	
	$(\sqrt{2}/20, 20)$	8.0770E-03	2.0433	6.7061E-01	0.9822
	$(\sqrt{2}/40, 40)$	1.9794E-03	2.0288	3.3666E-01	0.9942
	$(\sqrt{2}/50, 50)$	1.2597E-03	2.0252	2.6950E-01	0.9971

Table 11. Error behaviors with $h = \sqrt{2}/N$ and $\alpha_1 = 0.4$ in Example 6.2.

(α_2, α_3)	(h, N)	$\|u - u_h\|_{\tilde{L}^\infty(L^2)}$	Rates	$\|u - u_h\|_{\tilde{L}^\infty(H^1)}$	Rates
(0.3,0.1)	$(\sqrt{2}/10, 10)$	3.3591E-02		1.3244E+00	
	$(\sqrt{2}/20, 20)$	8.1935E-03	2.0355	6.7053E-01	0.9820
	$(\sqrt{2}/40, 40)$	2.0219E-03	2.0188	3.3665E-01	0.9941
	$(\sqrt{2}/50, 50)$	1.2904E-03	2.0125	2.6949E-01	0.9971
(0.3,0.2)	$(\sqrt{2}/10, 10)$	3.3538E-02		1.3245E+00	
	$(\sqrt{2}/20, 20)$	8.1763E-03	2.0363	6.7054E-01	0.9820
	$(\sqrt{2}/40, 40)$	2.0168E-03	2.0194	3.3665E-01	0.9941
	$(\sqrt{2}/50, 50)$	1.2869E-03	2.0132	2.6949E-01	0.9971

Table 12. Error behaviors with $N = 1000$ and $\alpha_1 = 0.8$ in Example 6.2.

(α_2, α_3)	h	$\|u - u_h\|_{\tilde{L}^\infty(L^2)}$	Rates	$\|u - u_h\|_{\tilde{L}^\infty(H^1)}$	Rates
(0.3,0.1)	$\sqrt{2}/10$	3.3500E-02		1.3244E+00	
	$\sqrt{2}/20$	8.1806E-03	2.0339	6.7053E-01	0.9820
	$\sqrt{2}/25$	5.2148E-03	2.0179	5.3736E-01	0.9922
	$\sqrt{2}/40$	2.0210E-03	2.0168	3.3665E-01	0.9950
(0.3,0.2)	$\sqrt{2}/10$	3.3461E-02		1.3245E+00	
	$\sqrt{2}/20$	8.1695E-03	2.0342	6.7054E-01	0.9820
	$\sqrt{2}/25$	5.2075E-03	2.0180	5.3736E-01	0.9922
	$\sqrt{2}/40$	2.0180E-03	2.0170	3.3665E-01	0.9950

Table 13. Error behaviors with $N = 1000$ and $\alpha_1 = 0.6$ in Example 6.2.

(α_2, α_3)	h	$\|u - u_h\|_{\tilde{L}^\infty(L^2)}$	Rates	$\|u - u_h\|_{\tilde{L}^\infty(H^1)}$	Rates
(0.3,0.1)	$\sqrt{2}/10$	3.3622E-02		1.3243E+00	
	$\sqrt{2}/20$	8.2161E-03	2.0329	6.7052E-01	0.9819
	$\sqrt{2}/25$	5.2385E-03	2.0169	5.3735E-01	0.9922
	$\sqrt{2}/40$	2.0317E-03	2.0152	3.3664E-01	0.9949
(0.3,0.2)	$\sqrt{2}/10$	3.3587E-02		1.3244E+00	
	$\sqrt{2}/20$	8.2063E-03	2.0331	6.7052E-01	0.9819
	$\sqrt{2}/25$	5.2322E-03	2.0170	5.3735E-01	0.9922
	$\sqrt{2}/40$	2.0292E-03	2.0152	3.3664E-01	0.9949

Table 14. Error behaviors with $N = 1000$ and $\alpha_1 = 0.4$ in Example 6.2.

(α_2, α_3)	h	$\|u - u_h\|_{\tilde{L}^\infty(L^2)}$	Rates	$\|u - u_h\|_{\tilde{L}^\infty(H^1)}$	Rates
(0.3,0.1)	$\sqrt{2}/10$	3.3712E-02		1.3242E+00	
	$\sqrt{2}/20$	8.2413E-03	2.0323	6.7050E-01	0.9818
	$\sqrt{2}/25$	5.2550E-03	2.0166	5.3734E-01	0.9922
	$\sqrt{2}/40$	2.0385E-03	2.0148	3.3664E-01	0.9949
(0.3,0.2)	$\sqrt{2}/10$	3.3680E-02		1.3243E+00	
	$\sqrt{2}/20$	8.2325E-03	2.0325	6.7051E-01	0.9819
	$\sqrt{2}/25$	5.2493E-03	2.0167	5.3735E-01	0.9922
	$\sqrt{2}/40$	2.0362E-03	2.0149	3.3664E-01	0.9949

Table 15. Error $\|u - u_h\|_{\tilde{L}^\infty(L^2)}$ with $h \approx \sqrt{2}N^{-(1-\alpha_1/2)}$ in Example 6.2.

$(\alpha_1, \alpha_2, \alpha_3)$	N	20	40	100	160
(0.8,0.3,0.1)	Error	9.4838E-02	4.1923E-02	1.2818E-02	7.3977E-03
	Rates		1.1777	1.2932	1.1696
(0.8,0.3,0.2)	Error	9.4742E-02	4.1867E-02	1.2798E-02	7.3860E-03
	Rates		1.1782	1.2935	1.1696
(0.6,0.3,0.1)	Error	5.2979E-02	1.9724E-02	5.2266E-03	2.6526E-03
	Rates		1.4255	1.4494	1.4430
(0.6,0.3,0.2)	Error	5.2919E-02	1.9698E-02	5.2191E-03	2.6487E-03
	Rates		1.4258	1.4495	1.4431
(0.4,0.3,0.1)	Error	2.7881E-02	9.1392E-03	2.0347E-03	9.6486E-04
	Rates		1.6091	1.6395	1.5874
(0.4,0.3,0.2)	Error	2.7846E-02	9.1268E-03	2.0318E-03	9.6350E-04
	Rates		1.6093	1.6395	1.5874

Table 16. Error $\|u - u_h\|_{\tilde{L}^\infty(H^1)}$ with $h \approx \sqrt{2}N^{-(1-\alpha_1)}$ in Example 6.2.

$(\alpha_1, \alpha_2, \alpha_3)$	N	5	8	10	14
(0.8,0.3,0.1)	Error	1.8606E+00	1.1100E+00	8.3659E-01	5.5991E-01
	Rates		1.0991	1.2671	1.1934
(0.8,0.3,0.2)	Error	1.8609E+00	1.1101E+00	8.3665E-01	5.5994E-01
	Rates		1.0993	1.2672	1.1935
(0.6,0.3,0.1)	Error	1.4658E+00	7.4450E-01	5.3752E-01	3.3671E-01
	Rates		1.4414	1.4598	1.3901
(0.6,0.3,0.2)	Error	1.4660E+00	7.4454E-01	5.3754E-01	3.3672E-01
	Rates		1.4415	1.4599	1.3901
(0.4,0.3,0.1)	Error	1.0254E+00	4.8024E-01	3.3669E-01	1.9830E-01
	Rates		1.6139	1.5915	1.5733
(0.4,0.3,0.2)	Error	1.0255E+00	4.8026E-01	3.3670E-01	1.9830E-01
	Rates		1.6140	1.5915	1.5734

From the above numerical experiments, although these two examples contain different fractional derivative terms and have different exact solutions, we can see that the convergence rates in the temporal direction are consistent with the theoretical results, and without considering the constraint condition $h \leq M_0/N$, the convergence rates in the spatial direction are also consistent with the theoretical results. These indicate that the proposed FVE method for the multi-term TFRD models with variable coefficients is feasible and effective.

Example 6.3. Consider the following two-term TFRD model

$$\begin{cases} \{D_t^{\alpha_1} + D_t^{\alpha_2}\}u(\boldsymbol{x},t) - \mathrm{div}(\mathcal{A}(\boldsymbol{x})\nabla u(\boldsymbol{x},t)) + q(\boldsymbol{x})u(\boldsymbol{x},t) = 0, & (\boldsymbol{x},t) \in \Omega \times J, \\ u(\boldsymbol{x},t) = 0, & (\boldsymbol{x},t) \in \partial\Omega \times J, \\ u(\boldsymbol{x},0) = u_0(\boldsymbol{x}), & \boldsymbol{x} \in \Omega, \end{cases} \tag{6.3}$$

where J, $q(\boldsymbol{x})$, and $\mathcal{A}(\boldsymbol{x})$ are same as in Example 6.1, the domain $\Omega = \{(x_1, x_2) \in \mathbb{R}^2 : x_1^2 + x_2^2 \leq 1\}$, and the initial data $u_0(\boldsymbol{x})$ is defined as follows:

$$u_0(\boldsymbol{x}) = 10(x_1^2 + x_2^2 - 1)^2 \sin(\pi x_1)\sin(\pi x_2), \ \boldsymbol{x} = (x_1, x_2) \in \Omega.$$

In this example, noting that Ω is a circular domain with a radius of 1, we should use the convex polygon to approximate this circular domain and perform triangular grid generation. Moreover, the source function $f = 0$, so it is difficult to obtain the exact solution of the model (6.3) due to the complexity of the domain Ω and initial data $u_0(\boldsymbol{x})$. For different fractional parameters $(\alpha_1, \alpha_2) = (0.8, 0.3), (0.4, 0.1)$, we conduct some experiments to observe the graphs of numerical solution at the final time $t = 1$ based on the different space-time grid partitions. In Figures 2(a) and 3(a), we take coarse space-time grid partitions $h = 0.1$ and $N = 10$, draw graphs of the numerical solutions and keep the grid lines. We next take more fine space-time grid partitions $h = 0.008$ and $N = 125$, and draw graphs of the numerical solutions in Figures 2(b) and 3(b). It can be observed that the graphs of numerical solutions obtained based on coarse and fine grids exhibit the same numerical behaviors, which also indicates that the numerical solutions tend to be stable as the grids become finer.

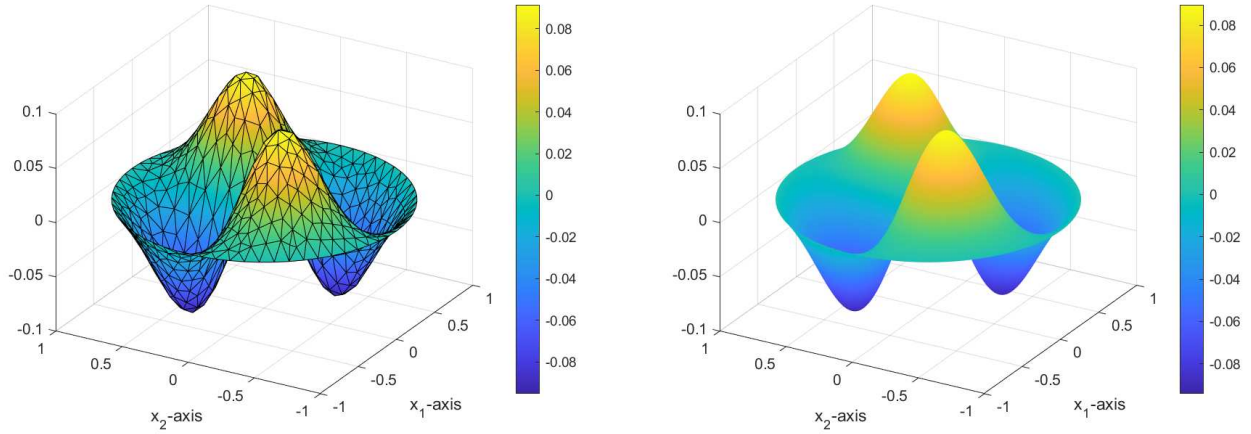

(a) $h = 0.1$, $N = 10$. (b) $h = 0.008$, $N = 125$.

Figure 2. Numerical solution of u at $t = 1$ with $\alpha_1 = 0.8$ and $\alpha_2 = 0.3$ based on different space-time grid partitions.

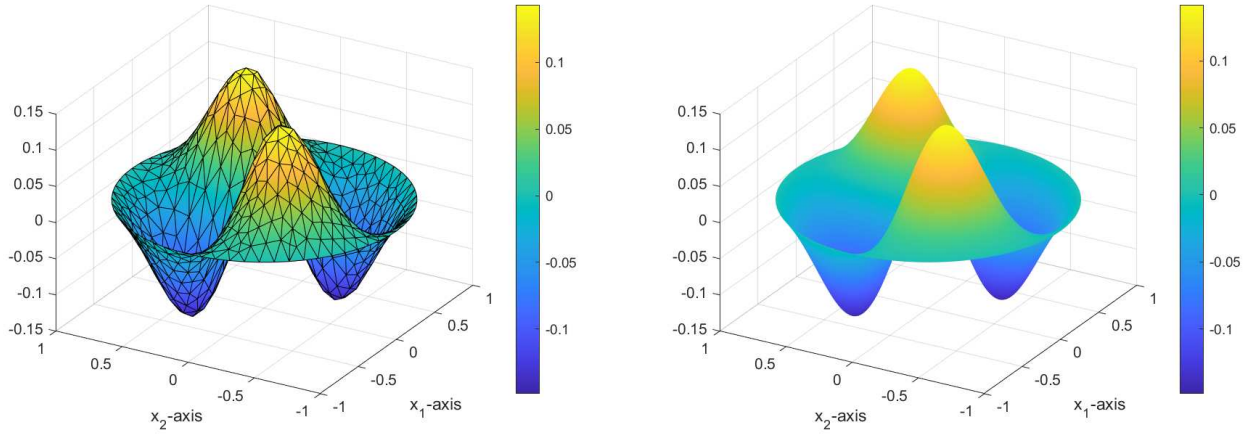

(a) $h = 0.1$, $N = 10$. (b) $h = 0.008$, $N = 125$.

Figure 3. Numerical solution of u at $t = 1$ with $\alpha_1 = 0.4$ and $\alpha_2 = 0.1$ based on different space-time grid partitions.

7. Conclusions

In this paper, we present an effective fully discrete FVE scheme based on the $L1$ formula to solve the multi-term TFRD models with variable coefficients by utilizing the interpolation operator Π_h^*. Within theoretical analysis, we use the matrix theories to demonstrate the existence and uniqueness of the discrete solution, and obtain the corresponding stability results and optimal error estimates in the discrete $L^\infty(L^2(\Omega))$ and $L^\infty(H^1(\Omega))$ norms by means of the multi-term fractional Gronwall inequality and a special technique. Moreover, from numerical results with different fractional derivative term, it can be seen that the convergence rates can still be maintained in practical calculations, even when the condition $h \le M_0/N$ fails to hold, which indicates that this condition is not necessary. In future works, we will continue to consider how to remove this constraint condition and apply the FVE method to solve more FDEs.

Author contributions

Jie Zhao: conceptualization, methodology, formal analysis, writing (original draft preparation), funding acquisition; Zhichao Fang: methodology, formal analysis, validation, software, writing (review and editing), project administration, supervision, funding acquisition; Jiahuan Ren: formal analysis, validation, writing (review and editing). All authors have read and agreed to the this version of the manuscript.

Use of Generative-AI tools declaration

The authors declare that they have not used Artificial Intelligence (AI) tools in the creation of this article.

Acknowledgments

This work was supported by the Natural Science Foundation of Inner Mongolia Autonomous Region (2024MS01013), the Scientific Research Projection of Higher Schools of Inner Mongolia Autonomous Region (NJZY23055), and the Central Government Guided Local Science and Technology Development Fund Project of China (2022ZY0175).

Conflict of interest

All authors declare no conflicts of interest in this paper.

References

1. N. F. Britton, *Reaction-diffusion equations and their applications to biology*, London: Academic Press, 1986.
2. P. Grindrod, *The theory and applications of reaction diffusion equations: patterns and waves*, 2 Eds., New York: Clarendon Press, 1996.
3. E. S. Baranovskii, R. V. Brizitskii, Z. Y. Saritskaia, Optimal control problems for the reaction-diffusion-convection equation with variable coefficients, *Nonlinear Anal.-Real*, **75** (2024), 103979. https://doi.org/10.1016/j.nonrwa.2023.103979
4. Y. C. Hua, Y. L. Tang, Z. H. Chen, Interpolated coefficient characteristic mixed finite element method for semilinear convection-diffusion optimal control problems, *J. Nonlinear Funct. Anal.*, **2024** (2024), 12. https://doi.org/10.23952/jnfa.2024.12
5. J. X. Cen, S. Migórski, C. Vetro, S. D. Zeng, Stability analysis for a contaminant convection-reaction-diffusion model of recovered fracturing fluid, *J. Nonlinear Var. Anal.*, **8** (2024), 581–600. https://doi.org/10.23952/jnva.8.2024.4.07
6. P. Paradisi, R. Cesari, F. Mainardi, F. Tampieri, The fractional Ficks law for non-local transport processes, *Physica A*, **293** (2001), 130–142. https://doi.org/10.1016/S0378-4371(00)00491-X
7. R. Metzler, J. Klafter, The random walks guide to anomalous diffusion: A fractional dynamics approach, *Physics Reports*, **339** (2002), 1–77. https://doi.org/10.1016/S0370-1573(00)00070-3
8. B. Ross, *Fractional calculus and its applications*, Berlin: Springer, 1975. https://doi.org/10.1007/BFb0067095
9. R. Hilfer, *Applications of fractional calculus in physics*, Singapore: World Scientific, 2000. https://doi.org/10.1142/3779
10. K. Diethelm, *The analysis of fractional differential equations*, Berlin: Springer, 2010. https://doi.org/10.1007/978-3-642-14574-2
11. P. J. Torvik, R. L. Bagley, On the appearance of the fractional derivative in the behavior of real materials, *J. Appl. Mech.*, **51** (1984), 294–298. https://doi.org/10.1115/1.3167615
12. C. Fetecau, M. Athar, C. Fetecau, Unsteady flow of a generalized Maxwell fluid with fractional derivative due to a constantly accelerating plate, *Comput. Math. Appl.*, **57** (2009), 596–603. https://doi.org/10.1016/j.camwa.2008.09.052

13. C. Y. Ming, F. W. Liu, L. C. Zheng, I. Turner, V. Anh, Analytical solutions of multi-term time fractional differential equations and application to unsteady flows of generalized viscoelastic fluid, *Comput. Math. Appl.*, **72** (2016), 2084–2097. https://doi.org/10.1016/j.camwa.2016.08.012

14. J. C. Ren, Z.-Z. Sun, Efficient numerical solution of the multi-term time fractional diffusion-wave equation, *E. Asian J. Appl. Math.*, **5** (2015), 1–28. https://doi.org/10.4208/eajam.080714.031114a

15. B. T. Jin, R. Lazarov, Y. K. Liu, Z. Zhou, The Galerkin finite element method for a multi-term time-fractional diffusion equation, *J. Comput. Phys.*, **281** (2015), 825–843. https://doi.org/10.1016/j.jcp.2014.10.051

16. A. H. Bhrawy, M. A. Zaky, A method based on the Jacobi tau approximation for solving multi-term time-space fractional partial differential equations, *J. Comput. Phys.*, **281** (2015), 876–895. https://doi.org/10.1016/j.jcp.2014.10.060

17. L. J. Qiao, D. Xu, Orthogonal spline collocation scheme for the multi-term time-fractional diffusion equation, *Int. J. Comput. Math.*, **95** (2018), 1478–1493. https://doi.org/10.1080/00207160.2017.1324150

18. F. H. Zeng, Z. Q. Zhang, G. E. Karniadakis, Second-order numerical methods for multi-term fractional differential equations: smooth and non-smooth solutions, *Comput. Method. Appl. M.*, **327** (2017), 478–502. https://doi.org/10.1016/j.cma.2017.08.029

19. Y. M. Zhao, Y. D. Zhang, F. Liu, I. Turner, Y. F. Tang, V. Anh, Convergence and superconvergence of a fully-discrete scheme for multi-term time fractional diffusion equations, *Comput. Math. Appl.*, **73** (2017), 1087–1099. https://doi.org/10.1016/j.camwa.2016.05.005

20. M. Li, C. M. Huang, W. Y. Ming, Mixed finite-element method for multi-term time-fractional diffusion and diffusion-wave equations, *Comp. Appl. Math.*, **37** (2018), 2309–2334. https://doi.org/10.1007/s40314-017-0447-8

21. Z.-Z. Sun, X. N. Wu, A fully discrete difference scheme for a diffusion-wave system, *Appl. Numer. Math.*, **56** (2006), 193–209. https://doi.org/10.1016/j.apnum.2005.03.003

22. Y. M. Lin, C. J. Xu, Finite difference/spectral approximations for the time-fractional diffusion equation, *J. Comput. Phys.*, **225** (2007), 1533–1552. https://doi.org/10.1016/j.jcp.2007.02.001

23. S. S. Ezz-Eldien, E. H. Doha, Y. Wang, W. Cai, A numerical treatment of the two-dimensional multi-term time-fractional mixed sub-diffusion and diffusion-wave equation, *Commun. Nonlinear Sci.*, **91** (2020), 105445. https://doi.org/10.1016/j.cnsns.2020.105445

24. Y. Q. Liu, H. G. Sun, X. L. Yin, L. B. Feng, Fully discrete spectral method for solving a novel multi-term time-fractional mixed diffusion and diffusion-wave equation, *Z. Angew. Math. Phys.*, **71** (2020), 21. https://doi.org/10.1007/s00033-019-1244-6

25. Y. H. Shi , Y. M. Zhao , F. L. Wang, Y. F. Tang, Superconvergence analysis of FEM for 2D multi-term time fractional diffusion-wave equations with variable coefficient, *Int. J. Comput. Math.*, **97** (2020), 1621–1635. https://doi.org/10.1080/00207160.2019.1639676

26. B. L. Yin, Y. Liu, H. Li, F. H. Zeng, A class of efficient time-stepping methods for multi-term time-fractional reaction-diffusion-wave equations, *Appl. Numer. Math.*, **165** (2021), 56–82. https://doi.org/10.1016/j.apnum.2021.02.007

27. M. F. She, D. F. Li, H. W. Sun, A transformed L1 method for solving the multi-term time-fractional diffusion problem, *Math. Comput. Simulat.*, **193** (2022), 584–606. https://doi.org/10.1016/j.matcom.2021.11.005

28. K. X. Li, H. Chen, S. S. Xie, Error estimate of L1-ADI scheme for two-dimensional multi-term time fractional diffusion equation, *Netw. Heterog. Media*, **18** (2023), 1454–1470. https://doi.org/10.3934/nhm.2023064

29. J. Zhao, S. B. Dong, Z. C. Fang, A mixed finite element method for the multi-term time-fractional reaction-diffusion equations, *Fractal Fract.*, **8** (2024), 51. https://doi.org/10.3390/fractalfract8010051

30. B. H. Lu, Z. P. Hao, C. Moya, G. Lin, FPINN-deeponet: A physics-informed operator learning framework for multi-term time-fractional mixed diffusion-wave equations, *J. Comput. Phys.*, **538** (2025), 114184. https://doi.org/10.1016/j.jcp.2025.114184

31. Y. H. Li, R. H. Li, Generalized difference methods on arbitrary quadrilateral networks, *J. Comput. Math.*, **17** (1999), 653–672.

32. R. H. Li, Z. Y. Chen, W. Wu, *Generalized difference methods for differential equations: numerical analysis of finite volume methods*, Boca Raton: CRC Press, 2000. https://doi.org/10.1201/9781482270211

33. J. L. Lv, Y. H. Li, Optimal biquadratic finite volume element methods on quadrilateral meshes, *SIAM J. Numer. Anal.*, **50** (2012), 2379–2399. https://doi.org/10.1137/100805881

34. K. Sayevand, F. Arjang, Finite volume element method and its stability analysis for analyzing the behavior of sub-diffusion problems, *Appl. Math. Comput.*, **290** (2016), 224–239. https://doi.org/10.1016/j.amc.2016.06.008

35. S. Karaa, K. Mustapha, A. K. Pani, Finite volume element method for two-dimensional fractional subdiffusion problems, *IMA J. Numer. Anal.*, **37** (2017), 945–964. https://doi.org/10.1093/imanum/drw010

36. S. Karaa, A. K. Pani, Error analysis of a FVEM for fractional order evolution equations with nonsmooth initial data, *ESAIM-Math. Model. Num.*, **52** (2018), 773–801. https://doi.org/10.1051/m2an/2018029

37. Z. C. Fang, R. X. Du, H. Li, Y. Liu, A two-grid mixed finite volume element method for nonlinear time fractional reaction-diffusion equations, *AIMS Mathematics*, **7** (2022), 1941–1970. https://doi.org/10.3934/math.2022112

38. T. X. Wang, Z. W. Jiang, A. L. Zhu, Z. Yin, A mixed finite volume element method for time-fractional damping beam vibration problem, *Fractal Fract.*, **6** (2022), 523. https://doi.org/10.3390/fractalfract6090523

39. Z. C. Fang, J. Zhao, H. Li, Y. Liu, Finite volume element methods for two-dimensional time fractional reaction-diffusion equations on triangular grids, *Appl. Anal.*, **102** (2023), 2248–2270. https://doi.org/10.1080/00036811.2022.2027374

40. Z. C. Fang, J. Zhao, H. Li, Y. Liu, A fast time two-mesh finite volume element algorithm for the nonlinear time-fractional coupled diffusion model, *Numer. Algor.*, **93** (2023), 863–898. https://doi.org/10.1007/s11075-022-01444-2

41. M. Donatelli, R. Krause, M. Mazza, K. Trotti, Multigrid for two-sided fractional differential equations discretized by finite volume elements on graded meshes, *J. Comput. Appl. Math.*, **444** (2024), 115787. https://doi.org/10.1016/j.cam.2024.115787

42. J. R. Zhang, Q. Yang, The finite volume element method for time fractional generalized Burgers' equation, *Fractal Fract.*, **8** (2024), 53. https://doi.org/10.3390/fractalfract8010053

43. J. Zhao, M. Cao, Z. C. Fang, A mixed finite volume element method for nonlinear time fractional fourth-order reaction-diffusion models, *Fractal Fract.*, **9** (2025), 481. https://doi.org/10.3390/fractalfract9080481

44. Z. C. Fang, J. Zhao, H. Li, Y. Liu, Fast two-grid finite volume element algorithms combined with Crank-Nicolson scheme for the nonlinear time fractional mobile/immobile transport model, *Int. J. Comput. Math.*, **2025** (2025), 1–22. https://doi.org/10.1080/00207160.2025.2507678

45. R. A. Adams, *Sobolev spaces*, New York: Academic Press, 1975.

46. R. Ewing, R. Lazarov, Y. P. Lin, Finite volume element aproximations of nonlocal reactive flows in porous media, *Numer. Meth. Part. D. E.*, **16** (2000), 285–311.

47. X. Wang, Y. H. Li, L^2 Error estimates for high order finite volume methods on triangular meshes, *SIAM J. Numer. Aanl.*, **54** (2016), 2729–2749. https://doi.org/10.1137/140988486

AIMS Press